HHS Public Access

Author manuscript

J Physiol. Author manuscript; available in PMC 2024 June 01.

Published in final edited form as:

J Physiol. 2023 June ; 601(12): 2513–2532. doi:10.1113/JP284004.

Novel Regenerative Drug, SPG302 Promotes Functional Recovery of Diaphragm Muscle Activity After Cervical Spinal Cord Injury

Matthew J. Fogarty[*], **Wen-Zhi Zhan**[*], **Vincent F. Simmon**[†], **Peter W. Vanderklish**[†], **Stella T. Sarraf**[†], **Gary C. Sieck, PhD**[*,#]

[*]Department of Physiology and Biomedical Engineering, Mayo Clinic, Rochester, Minnesota, USA

[†]Spinogenix Inc, 4225 Executive Square, Suite 600 La Jolla, California, USA

Abstract

Spinal cord hemisection at C_2 (C_2SH), sparing the dorsal column is widely used to investigate the effects of reduced phrenic motor neuron (PhMN) activation on diaphragm muscle (DIAm) function, with reduction in DIAm activity on the injured side during eupnoea. Following C_2SH, recovery of DIAm EMG activity may occur spontaneously over subsequent days/weeks. Various strategies have been effective at improving the incidence and magnitude of DIAm recovery during eupnoea, but little is known about the effects of C_2SH on transdiaphragmatic pressure (P_{di}) during other ventilatory and non-ventilatory behaviours. We employ SPG302, a novel type of pegylated benzothiazole derivative, to assess whether enhancing synaptogenesis (i.e., enhancing spared local connections) will improve the incidence and the magnitude of recovery of DIAm EMG activity and P_{di} function 14-days post C_2SH. In anesthetized Sprague Dawley rats, DIAm EMG and P_{di} were assessed during eupnoea, hypoxia/hypercapnoea and airway occlusion prior to surgery (C2SH or sham), immediately post-surgery and at 14-days post-surgery. In C_2SH rats, 14 days of DMSO (vehicle) or SPG302 treatments (IP injection) occurred. At the terminal experiment, maximum P_{di} was evoked by bilateral phrenic nerve stimulation. We show that significant EMG and P_{di} deficits are apparent in C_2SH compared to sham rats immediately after surgery. In C_2SH rats treated with SPG302, recovery of eupneic, HH and occlusion DIAm EMG was enhanced compared to vehicle rats after 14 days. Treatment with SPG302 also ameliorated Pdi deficits following C_2SH. In summary, SPG302 is an exciting new therapy to explore for use in spinal cord injuries.

[#]Correspondence: Gary C. Sieck, PhD, Vernon F. and Earline D. Dale Professor, Distinguished Investigator, Department of Physiology & Biomedical Engineering, Mayo Clinic, 200 1st St SW, Rochester, MN 55905, Phone: (507) 284 6850, sieck.gary@mayo.edu.

Author Contributions: All experiments were performed in the laboratory of Dr. Gary C. Sieck at Mayo Clinic. MJF, VSF, PV, STS and GCS participated in the conception of the studies. MJF and GCS designed the experiments. MJF and WZZ performed experiments. MJF, WZZ, and GCS analyzed and interpreted data. MJF drafted the manuscript. MJF and GCS created the Figures. All authors approved the final version of the manuscript and agree to be accountable for all aspects of the work in ensuring that questions related to the accuracy or integrity of any part of the work are appropriately investigated and resolved.

Competing Interests: VFS, PV and STS declare that they are members of the executive team and shareholders of Spinogenix. All other authors declare no competing interests.

Ethical approval and consent to participate: Approval from the Institutional Animal Care and Use Committee (IACUC) at Mayo Clinic (A00005858–00 and A00003105–17-R20) was obtained prior to all animal studies.

Consent for Publication: All authors approved the contents of this publication.

Graphical Abstract

Following a dorsal laminectomy, rats underwent a C_2 cervical hemisection surgery (C_2SH, surgical field inset) or sham (laminectomy only), severing the right-sided spinal projections of the lateral and ventral funiculus (grey portion of transverse spinal cord) and sparing the dorsal funiculus and the entire left side of C_2 (green portion of transverse spinal cord). Following C_2SH, rats were randomly assigned to either vehicle (DMSO-orange rats) or SPG302 (a novel pegylated benzothiazole derivatives-blue rats) treatments intraperitoneally for 14 days. Example diaphragm muscle (DIAm) RMS EMG on the injured side (grey) and uninjured (green) side from vehicle and SPG rats at 14-days post-C_2SH are shown on the right hand end of the top row of figures. 14 days post-C_2SH, DIAm RMS EMG, ventilatory transdiaphragmatic pressure (P_{di}), and maximum P_{di} (P_{dimax}), evoked via bilateral phrenic nerve stimulation, was compared to pre-injury values (within each rat) and across groups between sham, vehicle and SPG302 treated rats. SPG302 increased the % of rats exhibiting recovery from C_2SH compared to vehicle, with recovery defined as being >10% of the initial pre-injury DIAm RMS EMG during eupnoea. C_2SH depressed P_{dimax}, with SPG302 having improved P_{dimax} compared to vehicle treated. In conclusion, SPG302 presents a promising potential therapeutic for use in spinal cord injury.

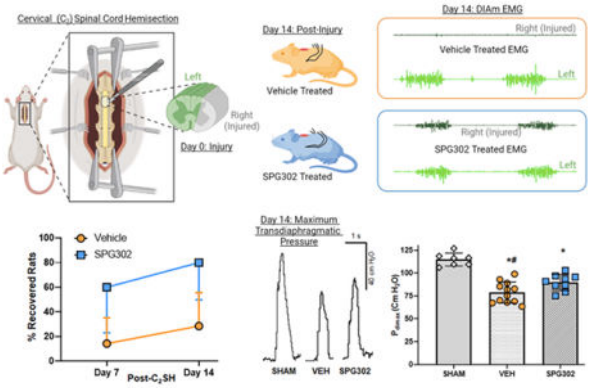

The Journal of Physiology

Keywords

diaphragm muscle; spinal cord injury; electromyography; transdiaphragmatic pressure; rehabilitation

INTRODUCTION

The diaphragm muscle (DIAm) is unique to mammals and is essential for ventilatory (breathing) and non-ventilatory behaviours, including cough, sneeze and straining maneuvers (Fogarty and Sieck, 2019). Neural control of the DIAm involves the orderly activation of motor units, comprising a phrenic motor neuron (PhMN) and the DIAm fibres it innervates, with DIAm motor units classified based on their mechanical and fatigue properties, and their fibre type composition (Fogarty and Sieck, 2019). The incessant

indefatigable requirement for ventilation is accomplished by recruitment of Slow (type S) and Fast Fatigue-Resistant (type FR) units, comprising smaller, more excitable (lower capacitance, higher input resistance) PhMNs innervating lower force-producing fatigue resistant type I and type IIa DIAm fibres, respectively (Sieck and Fournier, 1989;Geiger *et al.*, 2000). By contrast, higher pressure requiring expulsive and straining behaviours are accomplished by recruitment of Fast Fatigable (type FF) units, comprising larger, less excitable (higher capacitance, lower input resistance) PhMNs innervating higher force-producing fatigue resistant type IIx/IIb DIAm fibres (Sieck and Fournier, 1989;Geiger *et al.*, 2000). The overall functional gamut of DIAm behaviours, as measured by transdiaphragmatic pressure (P_{di}, the difference between thoracic and abdominal pressures) in rats is >10-fold, with marked differences between eupnoea, ~15 cm H_2O and maximum P_{di} (P_{dimax}, assessed via bilateral phrenic nerve stimulation) ~85–125 cm H_2O (Khurram *et al.*, 2018;Khurram *et al.*, 2019).

Descending ipsilateral bulbospinal glutamatergic inputs to PhMNs from the rostral ventral respiratory group (rVRG) are responsible for “inspiratory drive” and inspiratory-related DIAm activity (McCrimmon *et al.*, 1989;Lipski *et al.*, 1994;McCrimmon *et al.*, 1995;Fogarty *et al.*, 2018a). Following cervical spinal cord hemisection (C_2SH), removal of these excitatory inputs (Rana *et al.*, 2020b) results in absent/markedly reduced DIAm activity (Moreno *et al.*, 1992;Fuller *et al.*, 2006;Fuller *et al.*, 2008). However, there are also latent contralateral excitatory inputs to PhMNs, which may provide a substrate for neuroplasticity and spontaneous recovery of inspiratory-related DIAm activity (Mantilla *et al.*, 2013a;Martinez-Galvez *et al.*, 2016;Hernandez-Torres *et al.*, 2017). Our past studies found a marked reduction in glutamatergic synaptic input to all PhMNs following C_2SH, but more pronounced reduction in smaller PhMNs (Rana *et al.*, 2020b). We also found that recovery of inspiratory DIAm EMG following after C_2SH was enhanced by intrathecal administration of brain-derived neurotrophic factor (BDNF) (Sieck *et al.*, 2021). We also found that inhibition of the high affinity receptor for BDNF, tropomyosin receptor kinase B (TrkB), blunts spontaneous recovery of inspiratory-related DIAm activity after C_2SH. While these data suggest that PhMN postsynaptic mechanisms may underlie spontaneous recovery, it is also possible that presynaptic restoration of glutamatergic drive to PhMNs facilitates functional recovery after C_2SH.

SPG302 is a 3rd generation compound of a class of pegylated benzothiazole derivatives, which have been shown to restore synaptic density in Alzheimer’s disease and traumatic brain injury (Zhang *et al.*, 2019;Trujillo-Estrada *et al.*, 2021), with attendant physiological benefits – namely improving recovery of motor performance and cognition in rats (Zhang *et al.*, 2019) and performance of hippocampus-dependent memory tasks in a mouse model of Alzheimer’s disease (Trujillo-Estrada *et al.*, 2021). Earlier generations of pegylated benzothiazole derivatives were shown to increase post-synaptic spine densities and functional synapses via an F-actin cytoskeleton dependent mechanism (Cifelli *et al.*, 2016;Lee *et al.*, 2016;Zhang *et al.*, 2019). While the effect of SPG302 and prototype compounds on spinal cord injury remains unknown, prior studies demonstrate the importance of glutamatergic receptors in improving recovery following C_2SH (Mantilla *et al.*, 2012;ElMallah *et al.*, 2015;Gransee *et al.*, 2017;Rana *et al.*, 2020a;Wollman *et al.*, 2020)

and the presence of dendritic spines on spinal motor neurons (Bandaru *et al.*, 2015;Fogarty *et al.*, 2017b;2020b).

Although a reduction of inspiratory DIAm EMG activity following C_2SH has been demonstrated in several studies (Golder *et al.*, 2003;Fuller *et al.*, 2006;Martinez-Galvez *et al.*, 2016;Hernandez-Torres *et al.*, 2017), changes in P_{di} have not been systematically evaluated following C_2SH. After C_2SH, up to 50% of DIAm force generating capacity may be lost, which can certainly affect P_{di}. Furthermore, there may be deficits in the activation of chest wall muscles following C_2SH that alter chest wall compliance (Denton and McKinlay, 2009;Beth Zimmer *et al.*, 2015), which may also affect P_{di}. We hypothesize that 14-day treatment with SPG302, will improve recovery of inspiratory related DIAm EMG and P_{di} following C_2SH.

MATERIALS AND METHODS

Ethical approval:

All procedures were performed in accordance with the American Physiological Society's Animal Care Guidelines and the National Institutes of Health (NIH) guide for use and care of laboratory animals. These procedures were approved by the Institutional Animal Care and Use Committee (IACUC) at Mayo Clinic (A00005858–00 and A00003105–17-R20) and complied with the principles of the *Journal* outlined previously (Grundy, 2015). For three days following all procedures, animals were monitored for their level of discomfort a least three times per day. In this study, all animals exhibited no discomfort during recumbency, with normal feeding, drinking and stooling behaviours following surgeries.

Experimental animals:

A total of 33 adult male Sprague-Dawley (~370 g) obtained from Envigo (Indianapolis, IN) were used in the study. Rats were assigned to three groups, sham surgery (SHAM, n=7), C_2SH vehicle (VEH, n=14) and C_2SH SPG302-treated (SPG302 n=10). Based on previous studies, we anticipated that ~25% of the VEH animals would exhibit spontaneous recovery of inspiratory-related DIAm EMG during the 2-week post-C_2SH period, determined as an amplitude of >10% of the pre-surgery eupneic DIAm EMG activity (Mantilla *et al.*, 2013a;Gransee *et al.*, 2015;Martinez-Galvez *et al.*, 2016;Hernandez-Torres *et al.*, 2017;Sieck *et al.*, 2021;Brown *et al.*, 2022). In this study, we used male rats, due to their well-characterized recovery rates in past studies (Hernandez-Torres *et al.*, 2017;Sieck *et al.*, 2021;Brown *et al.*, 2022). Animals were acclimated for at least 1 week before surgery and maintained on an alternating 12:12 h light-dark cycle with *ad libitum* access to fresh water and rat chow. For all surgical procedures, anesthesia was administered via intraperitoneal injections of xylazine (10 mg/kg) and ketamine (80 mg/kg), with the adequacy of anaesthetic depth ensured by continual monitoring of the palpebral and pedal withdrawal reflexes. The sham control animals underwent the same surgical procedures (DIAm EMG electrode insertion, laminectomy), excluding C_2SH.

SPG302 Treatment:

Based on prior reports with SPG compounds (Zhang *et al.*, 2019;Trujillo-Estrada *et al.*, 2021), a dose of 30 mg/kg was used in the present study. SPG302 (gift from Spinogenix Inc., San Diego CA) was diluted in 0.3% DMSO and injected intraperitoneally each day for 14 days following C_2SH surgery (day 0). Prior to injection the site and needle was sanitized with an 75% ethanol, and upon puncture of the peritoneum, the plunger was withdrawn slightly to ensure there was no perforation of the vasculature. Vehicle treated rats were administered 3% DMSO in saline injected intraperitoneally for 14 days following C_2SH surgery, with rat treatment groups chosen randomly. Previous *in vitro* and *in vivo* studies show a relatively flat dose response to benzothiazole derivatives (Cifelli *et al.*, 2016;Zhang *et al.*, 2019). We specifically chose 30 mg/kg, as this had a potent effect of increasing the expression of PSD95 (Trujillo-Estrada *et al.*, 2021), which has been shown to be present on motor neurons (Fogarty *et al.*, 2013) and is involved in excitatory neurotransmission (Kennedy, 1997). *In vivo*, this SPG302 concentration dose is well tolerated in rodents for at least one month of intraperitoneal daily dosing (Trujillo-Estrada *et al.*, 2021). Following intraperitoneal dosing all rats were active and exploratory within their cage, exhibiting no overt signs of distress.

Diaphragm EMG activity:

Three days prior to sham or C_2SH surgery, under intraperitoneal anaesthesia with xylazine (10 mg/kg) and ketamine (80 mg/kg), with the adequacy of anaesthetic depth ensured by continual monitoring of the palpebral and pedal withdrawal reflexes, a pair of fine wire electrodes (~2 mm recording area) were implanted bilaterally into the mid-costal region of the DIAm to record chronic DIAm EMG activity, as previously described (Trelease *et al.*, 1982;Hernandez-Torres *et al.*, 2017;Khurram *et al.*, 2019). The EMG electrode wires were tunneled subcutaneously to the dorsum of the rat for repeated recordings. In anaesthetised animals (xylazine (10 mg/kg) and ketamine (80 mg/kg)), DIAm EMG activity was recorded during eupnoea, hypoxia/hypercapnoea (HH) and airway occlusion. DIAm EMG activity recorded immediately prior to C_2SH or sham surgeries was used as a baseline for subsequent analyses of DIAm EMG activity immediately after C_2SH and sham surgeries (day 0) and at day 3 (eupnoea only) and day 14 following surgery (Hernandez-Torres *et al.*, 2017;Sieck *et al.*, 2021). The magnitude of DIAm EMG activity was quantified as the cumulative root-mean-square (RMS) across the entire inspiratory burst divided by the burst duration. These analyses were performed on both the injured and uninjured sides of the DIAm. Respiratory rates and duty cycle were calculated using DIAm EMG in a manner identical to prior studies (Hernandez-Torres *et al.*, 2017;Sieck *et al.*, 2021;Brown *et al.*, 2022).

Transdiaphragmatic Pressure Measurements:

Transdiaphragmatic pressure (P_{di}) was measured as the difference between esophageal and gastric pressures as previously described (Sieck and Fournier, 1989;Khurram *et al.*, 2018;Fogarty *et al.*, 2022) under intraperitoneal anaesthesia with xylazine (10 mg/kg) and ketamine (80 mg/kg), with the adequacy of anaesthetic depth ensured by continual monitoring of the palpebral and pedal withdrawal reflexes. Briefly, two 3.5 French Millar solid-state pressure catheters (SPR-524; Millar Instruments, Houston, TX,

RRID:SCR_018840) were inserted through the mouth and into the esophagus and stomach. Correct catheter position was determined based on the direction of signal deflection during real-time measurements. Esophageal (P_{es}) and abdominal pressures (P_{gas}) were recorded and digitized (400 Hz) with PowerLab 4/35 and visualized in real-time with LabChart 8 (ADInstruments, Colorado Springs, CO, RRID:SCR_01755). From the P_{di} tracings peak amplitude, respiratory rate, inspiratory duration, and duty cycle were determined in a manner similar to previous reports (Sieck and Fournier, 1989;Khurram *et al.*, 2018;Fogarty *et al.*, 2022). During P_{di} measurements, the abdomen was bound to limit DIAm contraction and thereby approximate maximum isometric conditions (Sieck and Fournier, 1989).

Diaphragm Motor Behaviours:

At the time of surgery and at day 14 following C_2SH or sham surgery, the P_{di} generated during eupnoea, HH and airway occlusion was assessed. At day 3, only DIAm activity was evaluated for inclusion of C_2SH animals. In addition, at day 14 during the terminal experiment, under intraperitoneal anaesthesia with xylazine (10 mg/kg) and ketamine (80 mg/kg), with the adequacy of anaesthetic depth ensured by continual monitoring of the palpebral and pedal withdrawal reflexes, the phrenic nerves were isolated ventrally in the neck and stimulated bilaterally to evoke P_{dimax}. For bilateral phrenic nerve stimulation, two pairs of bipolar electrodes (125 μm platinum iridium wires with 0.5 mm inter-electrode spacing; FHC, #PBSD0875, Bowdoin, ME, RRID:SCR_018944) were used to stimulate (Grass S88 stimulator, RRID:SCR_016192) the phrenic nerves (0.05 ms duration ~10 mA pulses at a frequency of 100 Hz in a 330 ms duration train) (Khurram *et al.*, 2018;Khurram *et al.*, 2019). To avoid current spread, a mineral oil bath was created in the neck surrounding the isolated phrenic nerves.

Recovery of inspiratory related DIAm activity during anesthesia (xylazine (10 mg/kg) and ketamine (80 mg/kg)) was defined as eupneic activity >10% of pre-injury values (Figure 1), in accordance with prior studies in our and other labs (Moreno *et al.*, 1992;Fuller *et al.*, 2006;Fuller *et al.*, 2008;Mantilla *et al.*, 2013a;Gransee *et al.*, 2015;Martinez-Galvez *et al.*, 2016;Hernandez-Torres *et al.*, 2017;Sieck *et al.*, 2021;Brown *et al.*, 2022). For eupnoea, HH and airway occlusion, DIAm EMG was normalized to the pre-injury value for each behaviour (namely eupnoea, HH and occlusion).

During eupnoea and HH, the average magnitude of DIAm EMG activity and P_{di} was calculated for 10 breaths (during the final 2 min of a 5-min exposure to HH). During airway occlusion, the average magnitude of DIAm EMG activity and P_{di} generated was determined for 3–5 maximal efforts. During bilateral phrenic nerve stimulation, the average of 3 maximal evoked P_{di} was calculated to determine P_{dimax}. Following terminal procedures, the rats were euthanized via transcardial exsanguination, under deep intraperitoneal anaesthesia (xylazine (50 mg/kg) and ketamine (80 mg/kg)), with death confirmed by the extended absence of circulation and respiration.

To compare EMG activation and P_{dimax} across behaviours within animals, we normalized all data as a % of EMG_{max} or P_{dimax}. Normalization procedures were identical to those used prior studies (Mantilla *et al.*, 2011;Gill *et al.*, 2015), with EMG_{max} and P_{dimax} extrapolated for pre-injury values, assuming a linear increase of RMS EMG and P_{di} across behaviours

with increasing PhMN activation. Where it was not possible to assess EMG_{max} and P_{dimax}, occlusion P_{di} was considered to be 30% of P_{dimax} (Khurram *et al.*, 2018;Khurram *et al.*, 2019), with regression-based estimates of P_{dimax} in VEH (105.8 ± 7.1 cm H_2O) and SPG302 rats (107.4 ± 7.0 cm H_2O), resembling published data (Khurram *et al.*, 2018;Khurram *et al.*, 2019).

Cervical spinal cord hemisection surgery:

The surgical methods for C_2SH have been previously described in detail (Miyata *et al.*, 1995;Fuller *et al.*, 2006;Fuller *et al.*, 2008;Mantilla *et al.*, 2013a;Mantilla *et al.*, 2013b;Beth Zimmer *et al.*, 2015;Hernandez-Torres *et al.*, 2017;Rana *et al.*, 2020b;Streeter *et al.*, 2020). Under intraperitoneal anaesthesia with xylazine (10 mg/kg) and ketamine (80 mg/kg), with the adequacy of anaesthetic depth ensured by continual monitoring of the palpebral and pedal withdrawal reflexes a dorsal laminectomy at C_2 was performed. Subsequently, the C_2 spinal cord was cut using a surgical microknife, beginning anterior to the dorsal root entry zone fissure and proceeding ventrally taking care to preserve the right hand side dorsal funiculus, ~7 mm from the midline at the level of the dorsal subdura. The right lateral and ventral funiculi are severed in this particular lesion, sparing the dorsal column. Anatomical locations were aided with the use of a rat spinal cord atlas (Watson *et al.*, 2009). Following the completion of the day 14 post-C_2SH terminal procedures, a subset of rats (n=14) were perfused (~40 mL/min.) with saline followed by 4 % paraformaldehyde, the cervical spinal cord excised, frozen in OCT and crysectioned (horizontal orientation) at 70 μm, in a manner identical to prior studies. Sections were mounted in DPX and autofluorescence at 488 nm was used to image mosaics (10x objective NA 0.8) of the gross anatomy of the spinal cord using an Olympus Fluoview Microscope (FV1200, Olympus USA) (Gransee *et al.*, 2015). Lesion severity was quantified (both in real terms and as a % of the total spinal hemisphere radius) in recovered and non-recovered rats by assessing the spared distance between the central canal and the medial extent of the lesion cut. This area corresponds to the “equatorial” latitude of the spinal cord (i.e., its widest extent) (Watson *et al.*, 2009). Animals that did not have spinal cords assessed were euthanised via transcardial exsanguination under deep intraperitoneal anaesthesia (xylazine (50 mg/kg) and ketamine (80 mg/kg)), with death confirmed by the extended absence of circulation and respiration.

As in previous studies, DIAm EMG activity was monitored during surgery to ensure that rhythmic inspiratory activity on the right (lesioned) side of the DIAm disappeared during C_2SH surgery. Immediately after surgery, rats were administered subcutaneous carprofen (5 mg/kg) and buprenorphine (0.1 mg/kg). The efficacy of C_2SH was confirmed at day 3 by the absence of inspiratory related DIAm EMG activity under conditions of ketamine (80 mg/kg) anesthesia. Animals displaying inspiratory related DIAm EMG activity were excluded from the study following *a priori* inclusion criteria consistent with our previous studies (Miyata *et al.*, 1995;Prakash *et al.*, 1999;Mantilla *et al.*, 2013a;Mantilla *et al.*, 2013b;Martinez-Galvez *et al.*, 2016;Hernandez-Torres *et al.*, 2017;Rana *et al.*, 2020b;Sieck *et al.*, 2021;Brown *et al.*, 2022). A total of 2 rats were excluded from the study due to spontaneous day 3 recovery, with these rats euthanised via transcardial exsanguination under deep intraperitoneal anaesthesia (xylazine (50 mg/kg) and ketamine (80 mg/kg)), with death confirmed by the extended absence of circulation and respiration.

Statistical analyses:

Prism 9 was used for all statistical analyses (Graphpad, Carlsbad, CA). The data sets were assessed for normality with D'Agostino and Pearson tests. Data exclusion was based on *a priori* criteria of being outside a range of two times the standard deviation away from the mean. We were powered to detect a significant difference of >20% in DIAm EMG amplitude and P_{di} across behaviours, and a >20% change in P_{dimax}. Student's unpaired *t*-test, one-way, matched two-way or three-way ANOVAs were performed on the measured variables with the following grouping factors: surgery (C_2SH vs sham), time (pre-surgery and day 0, 3 and 14 post-surgery), and treatment (vehicle or SPG302). When appropriate within group differences were evaluated using Tukey's or Bonferroni *post hoc* tests. Data was reported in the Results and Figures as the mean ± the standard deviation of the mean. Statistical significance was set at $P<0.05$, with P values reported to three significant figures in the results.

RESULTS

C_2SH severely reduced unilateral DIAm EMG activity during eupnoea, HH and occlusion

The amplitude of DIAm EMG activity was assessed during eupnoea, HH and airway occlusion before and immediately after C_2SH (VEH: $n=14$; SPG302: $n=10$) or sham surgery (SHAM: $n=7$) in all rats (Figure 1). As expected, C_2SH resulted in a stark reduction of DIAm EMG activity during eupnoea and occlusion on the ipsilateral side to injury, compared to initial RMS EMG normalized to the pre-injury value for each behaviour (Figure 1). Notably, in all rats, DIAm RMS EMG increased across behaviours, with eupnoea < HH < occlusion (Figure 1). In SHAM control rats, DIAm EMG activity was equivalent on both left and right sides and unaffected by surgery across all behaviours (eupnoea: 107.5 ± 9.4 %; HH: 105.9 ± 10.3 %; occlusion: 107 ± 11.6 %; Figure 1). At 14 days post-surgery, DIAm EMG activity on the left side of the DIAm in C_2SH (VEH: 104.2 ± 18 %; SPG302: 108.2 ± 33 %) and SHAM (105.2 ± 33 %) rats was equivalent.

SPG302 increases incidence of recovery in DIAm EMG activity following C_2SH

The C_2SH lesion we employ in the present study is highly characterized structurally (Figure 2A) and functionally (i.e., with EMG inclusion/exclusion criteria during C_2SH and 3 days post-C_2SH) (Miyata *et al.*, 1995;Prakash *et al.*, 1999;Mantilla *et al.*, 2013a;Mantilla *et al.*, 2013b;Martinez-Galvez *et al.*, 2016;Hernandez-Torres *et al.*, 2017;Rana *et al.*, 2020b;Sieck *et al.*, 2021;Brown *et al.*, 2022). We have previously documented progressive spontaneous recovery (i.e., a return to >10% of pre-injury DIAm EMG on the lesioned side) in ~25% or male rats in the weeks following C_2SH lesions (Mantilla *et al.*, 2013a;Gransee *et al.*, 2015;Martinez-Galvez *et al.*, 2016;Hernandez-Torres *et al.*, 2017;Sieck *et al.*, 2021;Brown *et al.*, 2022). Treatment with SPG302 significantly increased the likelihood of recovery at 7-days (60% recovery; $P=0.0323$, Fisher's exact test) and 14-days (80% recovery; $P=0.0361$, Fisher's exact test) following C_2SH, compared to VEH rats (15% recovery at 7-days and 29% recovery at 14-days post C_2SH; Figure 2B). Overall, by 14 days, SPG302 treated rats were ~2.5 times more likely to have recovered DIAm EMG activity (odds ratio 10.0; Figure 2B).

Lesion extent did not influence the likelihood of recovery in either SPG302 or VEH rats (Figure 2C), with the spared portion (central canal to lesion edge) of the spinal cord at the middle "equatorial" latitude of C_2 region being unchanged between non-recovered (454 ± 91 μm, n=7) and recovered rats (431 ± 113 μm, n=7; P=0.687, Student's unpaired t-test; Figure 2D). Expressed as a % of the spinal cord radius at the "equatorial" latitude of C_2, we observed no differences in the spared region between non-recovered (24.8 ± 4.2 %, n=7) and recovered rats (24.3 ± 5.8 %, n=7; P=0.855, Student's unpaired t-test; Figure 2E). Note that these spared portions are in addition to the spared dorsal columns.

SPG302 increases the magnitude of recovery of ventilatory EMG activity during eupnoea, HH and occlusion following C_2SH

Immediately prior to C_2SH surgery, immediately following C_2SH and 14 days following surgeries we assessed DIAm RMs EMG during eupnoea, HH and occlusion (Figure 3). Following C_2SH, treatment with SPG302 improved the DIAm EMG compared to VEH rats, with EMG dependent on behaviour ($F_{(2,44)}$=16.7, P<0.0001), treatment ($F_{(1,44)}$=7.0, P=0.0217), time post-injury ($F_{(1,22)}$=31.4, P<0.0001) and the interaction between time and treatment ($F_{(1,44)}$=10.2, P=0.0045, Three-way ANOVA; Figure 3).

During eupnoea, DIAm EMG immediately following injury was no different between VEH (4.8 ± 2.2 %) and SPG302 rats (4.0 ± 1.5 %; P>0.99; Figure 3). At 14 days post injury, there was no significant increase in DIAm EMG in VEH rats (10.9 ± 7.6 %) compared to immediately following injury (P>0.99; Figure 3). However, in SPG302 treated rats, DIAm EMG was increased by > 10-fold after 14 days (47.4 ± 30.3 %; P=0.0005; Figure 3). In addition, DIAm EMG activity during eupnoea was increased by ~4-fold by SPG302 treatment compared to VEH rats at day 14 (P=0.0013; Figure 3).

During HH, DIAm EMG immediately following injury was no different between VEH (5.8 ± 2.7 %) and SPG302 rats (4.0 ± 1.7 %; P>0.99; Figure 3). At 14 days post injury, there was no significant increase in DIAm EMG in VEH rats (17.8 ± 14.9 %) compared to immediately following injury (P>0.99; Figure 3). However, in SPG302 rats, DIAm EMG was increased by > 12-fold after 14 days (50.1 ± 33.4 %; P=0.0002; Figure 3). In addition, DIAm EMG activity during HH was increased by > 3-fold by SPG302 treatment compared to VEH rats at day 14 (P=0.0024; Figure 3).

During occlusion, DIAm EMG immediately following injury was no different between VEH (20.1 ± 19.6 %) and SPG302 rats (16.5 ± 10.7 %; P>0.99; Figure 3). At 14 days post injury, there was no significant increase in DIAm EMG in VEH rats (41.3 ± 31.7 %) compared to immediately following injury (P=0.674; Figure 3). However, in SPG302 rats, DIAm EMG was increased by > 3.5-fold after 14 days (57.9 ± 39.0 %; P=0.0013; Figure 3).

In recovered rats, DIAm EMG activity during eupnoea was increased in SPG302 treated rats compared to VEH treated rats.

In the subset of rats that exhibited recovery (i.e., >10% of initial eupneic DIAm RMS EMG), EMG was dependent on treatment ($F_{(1,10)}$=7.3, P=0.0220), time ($F_{(1,10)}$=28.1, P=0.0003), and the interaction between treatment and time ($F_{(1,10)}$=9.1, P=0.0128, Two-way ANOVA; Figure 4). Immediately post C_2SH surgery, there was no difference between

SPG302 (3.8 ± 1.2, n=8) and VEH (5.7 ± 1.4, n=4) rat DIAm RMS EMG during eupnoea (P>0.99, Bonferroni *post hoc* test; Figure 4). At 14 days post C_2SH, DIAm RMS EMG was ~3-fold greater in SPG302 rats (58.6 ± 24.7 % of initial), compared to spontaneously recovered VEH controls (20.0 ± 9.7 % of initial; P=0.001, Bonferroni *post hoc* test; Figure 4).

Ventilatory P_{di} deficits following C_2SH are ameliorated with SPG302

We assessed P_{di} under anaesthetized conditions in SHAM (n=7), VEH (n=13) and SPG302 (n=9) rats immediately prior to and immediately after surgical procedures (sham or C_2SH) and 14 days after surgery. Eupneic P_{di} was dependent on treatment ($F_{(2,26)}$=6.5, P=0.005), time ($F_{(2,52)}$=30.8, P<0.0001) and the interaction between treatment and time ($F_{(4,52)}$=6.4, P=0.0003, Two-Way ANOVA; Figure 5). Bonferroni post-tests show unchanged eupnoea P_{di} between all experimental groups at day 0 prior to surgery (SHAM: 14.9 ± 3.6 cm H_2O; VEH: 13.2 ± 3.5 cm H_2O; SPG302: 15.0 ± 4.5 cm H_2O; P>0.64 in all combinations; Figure 5). Immediately following C_2SH (day 0), eupnoea P_{di} was reduced by ~49% in VEH (7.4 ± 1.0 cm H_2O; P<0.0001) and by ~43% in SPG302 rats (8.3 ± 2.0 cm H_2O; P=0.0007) compared to SHAM rats (14.5 ± 4.5 cm H_2O; Figure 5). There was no difference in eupnoea P_{di} between VEH and SPG302 immediately following C_2SH (P>0.99). After 14 days post C_2SH, eupnoea P_{di} remained reduced by ~34% in VEH rats (9.5 ± 2.8 cm H_2O; P=0.0042), whereas eupnoea P_{di} in SPG302 treated rats (12.9 ± 2.6 cm H_2O; P=0.968) was not different from SHAM (14.5 ± 3.7 cm H_2O; Figure 5). Additionally, SPG302 treatment improved eupnoea P_{di} at day 14 by ~36% compared to VEH (P=0.0329, Figure 5).

HH P_{di} was dependent on treatment ($F_{(2,26)}$=5.0, P=0.015), time ($F_{(2,52)}$=32.8, P<0.0001) and the interaction between treatment and time ($F_{(4,52)}$=6.7, P=0.0002, Two-Way ANOVA; Figure 6). Bonferroni post-tests show unchanged HH P_{di} between all experimental groups at day 0 prior to surgery (SHAM: 15.8 ± 3.7 cm H_2O; VEH: 14.0 ± 3.6 cm H_2O; SPG302: 15.6 ± 3.7 cm H_2O; P>0.820 in all combinations; Figure 6). Immediately following C_2SH (day 0), HH P_{di} was reduced by ~44% in VEH treated rats (8.3 ± 2.7 cm H_2O; P=0.0008) and by ~49% in SPG302 treated rats (7.5 ± 1.8 cm H_2O; P=0.0004) compared to SHAM rats (14.5 ± 4.2 cm H_2O; Figure 6). There was no difference in HH P_{di} between VEH and SPG302 treated rats immediately following C_2SH (P>0.99). After 14 days post C_2SH, HH P_{di} remained reduced by ~33% in VEH treated rats (10.0 ± 3.1 cm H_2O; P=0.0089), whereas HH P_{di} in SPG302 treated rats (14.0 ± 4.5 cm H_2O; P>0.99) was not different compared to SHAM treated rats (14.9 ± 4.2 cm H_2O; Figure 6). Additionally, SPG302 treatment improved HH P_{di} at day 14 by ~40% compared to VEH treatment (P=0.0269, Figure 6) in C_2SH rats.

Occlusion P_{di} was dependent on treatment ($F_{(2,26)}$=12.9, P=0.0001), time ($F_{(2,52)}$=36.8, P<0.0001) and the interaction between treatment and time ($F_{(4,52)}$=8.5, P<0.0001, Two-Way ANOVA; Figure 7). Bonferroni post-tests show unchanged occlusion P_{di} between all experimental groups at day 0, prior to surgery (SHAM: 34.9 ± 3.6 cm H_2O; VEH: 33.0 ± 4.8 cm H_2O; SPG302: 34.7 ± 4.9 cm H_2O; P>0.99 in all combinations; Figure 7). Immediately following C_2SH (day 0), occlusion P_{di} was reduced by ~46% in VEH treated rats (18.7 ± 5.8 cm H_2O; P<0.0001) and by ~47% in SPG302 treated rats (18.4 ± 5.3 cm

H_2O; P<0.0001) compared to SHAM rats (34.5 ± 4.1 cm H_2O; Figure 7). There was no difference in occlusion P_{di} between VEH and SPG302 treated rats immediately following C_2SH (P>0.99). After 14 days post C_2SH, occlusion P_{di} remained reduced by ~31% in VEH rats (24.4 ± 6.3 cm H_2O; P=0.0001), whereas occlusion P_{di} in SPG302 rats (30.3 ± 7.4 cm H_2O; P=0.191) was not different compared to SHAM treatment (35.4 ± 4.9 cm H_2O; Figure 7). Additionally, SPG302 treatment improved occlusion P_{di} at day 14 by ~30% compared to VEH treatment (P=0.0453, Figure 7).

P_{dimax} deficits following C_2SH are ameliorated with SPG302

Bilateral phrenic nerve stimulations were used to determine P_{dimax} in a manner identical to previous studies in rats (Figure 8). P_{dimax} was dependent on treatment ($F_{(2,25)}$=30.6, P<0.0001, One-way ANOVA), with Tukey's post-tests showing that C_2SH reduced P_{dimax} in VEH treated rats (78.7 ± 11.5 cm H_2O; P<0.0001) and SPG302 treated rats (89.8 ± 8.8 cm H_2O; P<0.0001) compared to SHAM treatment (114.8 ± 7.1 cm H_2O; Figure 8) by ~31% and ~22%, respectively. In addition, compared to VEH treated rats, treatment with SPG302 increased P_{dimax} following C_2SH by ~14% (P=0.0419; Figure 8).

SPG302 improves the EMG and Pdi of ventilatory and non-ventilatory behaviours in C2SH rats

As previously observed (Mantilla *et al.*, 2011;Gill *et al.*, 2015), there was a strong correlation between P_{di} and RMS EMG measures across ventilatory and non-ventilatory behaviours in VEH (r^2>0.99) and SPG302 (r^2=0.98) treated rats (Figure 9). Cluster analysis shows discrete groups of VEH and SPG302 values across all behaviours, with the XY relationships of EMG and P_{di} (normalized to EMG_{max} and P_{dimax}, respectfully) after 14 days of C_2SH (Figure 9). In all behaviours, the EMG and P_{di} values of VEH rats are reduced compared to those treated with SPG302.

Effects of C_2SH on respiratory rate and occlusion during eupnoea, HH and occlusion

During eupnoea, there was no effect of time ($F_{(2,56)}$=0.9, P=0.396), group (i.e., surgery/treatment; $F_{(2,28)}$=0.3, P=0.750) or interaction between time and group ($F_{(4,56)}$=1.1, P=0.379) on respiratory rate, with eupnoea respiratory rates ~55 breaths/minute in all groups pre- and post-surgery (Two-Way ANOVA; Table 1). Likewise, the duty cycle of eupnoea was unaffected by time ($F_{(2,56)}$=1.6, P=0.212), group ($F_{(2,28)}$=0.2, P=0.790) or interaction between time and group ($F_{(4,56)}$=0.3, P=0.863) on respiratory rate, with eupnoea duty cycle ~42 % in all groups pre- and post-surgery (Two-Way ANOVA; Table 1).

During HH, there was no effect of time ($F_{(2,56)}$=2.0, P=0.124), group ($F_{(2,28)}$=0.1, P=0.880) or interaction between time and group ($F_{(4,56)}$=1.3, P=0.297) on respiratory rate, with HH respiratory rates ~70–75 breaths/minute in all groups pre- and post-surgery (Two-Way ANOVA; Table 1). Likewise, the duty cycle of HH was unaffected by time ($F_{(2,56)}$=0.4, P=0.678), group ($F_{(2,28)}$=0.1, P=0.880) or interaction between time and group ($F_{(4,56)}$=1.5, P=0.206) on respiratory rate, with eupnoea duty cycle ~50 % in all groups pre- and post-surgery (Two-Way ANOVA; Table 1).

During occlusion, there was no effect of time ($F_{(2,56)}$=1.1, P=0.356), group ($F_{(2,28)}$=0.5, P=0.610) or interaction between time and group ($F_{(4,56)}$=0.6, P=0.694) on respiratory rate, with occlusion respiratory rates ~35 breaths/minute in all groups pre- and post-surgery (Two-Way ANOVA; Table 1). Likewise, the duty cycle of occlusion was unaffected by time ($F_{(2,56)}$=0.4, P=0.646), group ($F_{(2,28)}$=0.4, P=0.694) or interaction between time and group ($F_{(4,56)}$=0.4, P=0.804) on respiratory rate, with eupnoea duty cycle ~40 % in all groups pre- and post-surgery (Two-Way ANOVA; Table 1).

Effects of C_2SH on the DIAm EMG of the unaffected side

At all time points and during all ventilatory behaviours (i.e., eupnoea, HH and airway occlusion), DIAm EMG of the uninjured side (ie., contralateral to the lesion) was recorded and analysed in the same manner as that of the injured side (Table 2). We did not observe any robust or systematic changes in DIAm EMG from the uninjured side with regard to time ($F_{(1,22)}$=2.2, P=0.152), behaviour ($F_{(2,44)}$=0.3, P=0.711), treatment ($F_{(1,22)}$=0.02, P=0.877), or the interaction between time and treatment ($F_{(1,22)}$=0.1, P=0.818; Three-Way ANOVA; Table 2).

DISCUSSION

This study presents four novel findings in C_2SH-lesioned rats: (i) C_2SH causes marked EMG deficits across ventilatory behaviours; (ii) C_2SH causes significant impairments in DIAm P_{di} during eupnoea, HH, occlusion and P_{dimax}; (iii) 14-day treatment with SPG302 following C_2SH significantly increases the incidence and magnitude of DIAm EMG recovery and (iv) ameliorated DIAm P_{di} deficits across ventilatory and non-ventilatory behaviours. Overall, this study ushers in a new approach towards restoring DIAm function following cervical spinal cord injury by enhancing synaptogenesis utilizing pegylated benzothiazole derivatives, such as SPG302. In addition to our innovative use of SPG302, we are the first to characterize P_{di} across a variety of ventilatory and non-ventilatory behaviours at various timepoints following C_2SH.

Many facets of the C_2SH lesion have been extremely well characterized, including the interruption of descending glutamatergic inspiratory drive (Tai and Goshgarian, 1996;Fogarty and Sieck, 2020;Rana *et al.*, 2020b), which is primarily ipsilateral (McCrimmon *et al.*, 1989;Lipski *et al.*, 1994;McCrimmon *et al.*, 1995). The unilateral lesioning of descending inputs during C_2SH abolishes ipsilateral DIAm EMG activity during eupnoea (Miyata *et al.*, 1995). Following C_2SH, DIAm EMG deficits have been routinely observed during some ventilatory behaviours, but not during maximum efforts and not normalized within behaviours. Indeed, the preponderance of past studies normalize to eupnoea, or sigh, (which is defined as a multiple of eupnoea) (Mantilla *et al.*, 2011;Martinez-Galvez *et al.*, 2016;Khurram *et al.*, 2018). In the present study, we normalized all data to the values obtained immediately prior to C2SH or sham surgery *within each behaviour*. Immediately following C_2SH, DIAm EMG activity was markedly reduced compared to initial pre-surgery EMG during eupnoea (~4–5% in VEH and SPG302 rats), HH (~4–6% in VEH and SPG302 rats) and occlusion (~17–20% in VEH and SPG302 rats). These deficits were consistent with reductions in DIAm EMG activity

reported for eupnoea (Mantilla *et al.*, 2013a;Gransee *et al.*, 2015;Martinez-Galvez *et al.*, 2016;Hernandez-Torres *et al.*, 2017;Sieck *et al.*, 2021;Brown *et al.*, 2022). In spontaneously recovered rats, DIA EMG is restored to ~25% of the initial level (Gransee *et al.*, 2013;2015). In previous studies where all DIAm EMG values were normalized to pre-surgery eupnoea, DIAm EMG during HH and occlusion was unchanged at 21 days (Martinez-Galvez *et al.*, 2016), although other groups have observed substantial depression of DIAm EMG during occlusion (Warren *et al.*, 2018). In VEH treated rats following C_2SH, we observed DIAm EMG (normalized to pre-surgery RMS EMG within each behaviour) values of ~10, 15 and 40% for eupnoea, HH and occlusion, respectively, regardless of recovery status (i.e., all recovered animals included in the data set). Excluding recovered rats, the DIAm EMG activity declines to ~7, 13 and 26% for eupnoea, HH and occlusion, respectively. In addition to characterizing DIAm EMG across different behaviours, our within-behaviour normalization approach reduced any intra-animal variability in past assessments normalizing to eupnoea. Our prior study showing significant reduction (~40%) in the co-efficient of variation by normalizing to behaviours other than eupnoea underlines the importance of appropriate normalization (Mantilla *et al.*, 2011).

Difficulties engendered by the variability of chronic DIAm EMG following C_2SH have led to integrative DIAm functional assessments of using plethysmography and arterial blood gases (Golder *et al.*, 2003;Fuller *et al.*, 2006;Warren *et al.*, 2018) or *ex vivo* approaches assessing DIAm contractility (Mantilla *et al.*, 2013b). Indeed, C_2SH reduced tidal volumes during eupnoea and augmented breaths in unanesthetized rats (Fuller *et al.*, 2006;Fuller *et al.*, 2008). However, these approaches are limited in scope and are not as well suited as P_{di} to estimate DIAm function across the range of ventilatory and non-ventilatory behaviours (Bellemare *et al.*, 1986;Sieck and Fournier, 1989;Fogarty and Sieck, 2019). The present study substantially expands the scope of functional DIAm assessment compared to previous efforts from within our lab and others by investigating C_2SH-induced changes in P_{di}. Using P_{di}, eupneic values are consistently ~10–15% of P_{dimax} in rodents ~110 cm H_2O (Khurram *et al.*, 2018;Khurram *et al.*, 2019;Fogarty *et al.*, 2022) and humans ~200 cm H_2O (Bellemare and Bigland-Ritchie, 1984;Aubier *et al.*, 1985;Bellemare *et al.*, 1986). Consistent with declines in tidal volumes with C_2SH, we observed reduced Pdi during eupnoea (~35%), HH (~35%) and occlusion (~35%) immediately following C_2SH, that persist until 14 days post-injury in VEH treated rats. In addition, we observed marked deficits in P_{dimax} following C_2SH, with VEH reduced by ~30% compared to SHAM treated rats. Thus, functional deficits following C_2SH are apparent across ventilatory and non-ventilatory behaviours, although the effects on endurance behaviours (eupnoea and HH) seem greater than effects on higher-pressure behaviours (occlusion and P_{dimax}). This result is consistent with a 60% reduction in glutamatergic inputs to smaller PhMNs (recruited for ventilatory activities (Sieck and Fournier, 1989;Fogarty and Sieck, 2019)) and an ~30% reduction in larger PhMNs (recruited for non-ventilatory behaviours (Sieck and Fournier, 1989;Fogarty and Sieck, 2019)), following C_2SH (Rana *et al.*, 2020b). In the present study we did not observe any changes in respiratory rate nor duty cycle across ventilatory activities, consistent with past reports (Hernandez-Torres *et al.*, 2017;Sieck *et al.*, 2021;Brown *et al.*, 2022).

Previous studies have shown P_{di} deficits and DIAm weakness are dependent upon the level of dissociation between of PhMNs and their constituent DIAm fibres. Namely,

denervation (severing of the phrenic nerve (Paterson, 1965)), C_4 contusion injury (with frank obliteration of ~30% of PhMNs (Alvarez-Argote *et al.*, 2016)), early onset hypertonia (with ~30% PhMN death (Brandenburg *et al.*, 2020)) and aging (with ~25% PhMN death (Fogarty *et al.*, 2018b)) all present with reduced DIAm isometric force and/or P_{dimax} (Gill *et al.*, 2015;Khurram *et al.*, 2018;Khurram *et al.*, 2019;Fogarty *et al.*, 2022). By contrast, mild frank DIAm weakness has only been observed following extended (42-days) intervals post-C_2SH (Mantilla *et al.*, 2013b). In our study, reduced P_{di} function across multiple behaviours may be related to either impaired activation or increased chest wall compliance during inspiration. We have extensive evidence (including in this study) that reduced PhMN activation is particularly apparent during ventilatory activities (Mantilla *et al.*, 2013a;Gransee *et al.*, 2015;Martinez-Galvez *et al.*, 2016;Hernandez-Torres *et al.*, 2017;Sieck *et al.*, 2021;Brown *et al.*, 2022). By contrast, increased chest wall compliance due to C_2SH-related impairment of the chest wall musculature (intercostals) that stiffens the thorax during inspiration (Denton and McKinlay, 2009;Beth Zimmer *et al.*, 2015), may impair P_{dimax} without requiring DIAm weakness *per se*.

Extensive research by assorted research groups shows spontaneous recovery of DIAm EMG activity during eupnoea may occur in the days following C_2SH (Goshgarian *et al.*, 1991;Moreno *et al.*, 1992;Miyata *et al.*, 1995;Fuller *et al.*, 2006;Fuller *et al.*, 2008;Singh *et al.*, 2012;Mantilla *et al.*, 2013a;Mantilla *et al.*, 2013b;Gransee *et al.*, 2015;Martinez-Galvez *et al.*, 2016;Gransee *et al.*, 2017;Hernandez-Torres *et al.*, 2017;Sieck *et al.*, 2021;Brown *et al.*, 2022). This improvement is likely related to both presynaptic and postsynaptic mechanisms strengthening spared connections (Fogarty and Sieck, 2020). Determining the locus of these spared pathways has generated considerable research interest, although differentiating the precise contributions of strengthened of contralateral descending, local segmental or ascending pre-synaptic inputs to PhMN has remained elusive (Porter, 1895;Streeter *et al.*, 2017;Streeter *et al.*, 2020;Sunshine *et al.*, 2020). In addition, potent postsynaptic intrinsic and active PhMN mechanisms may precipitate recovery following C_2SH. Indeed, enhanced expression of postsynaptic glutamate receptor subtypes or serotonin activation may improve the intrinsic amplification of residual inspiratory drive from these spared inputs (Hadley *et al.*, 1999;Zhou and Goshgarian, 1999;Mantilla *et al.*, 2012;Gransee *et al.*, 2017). Collateral branching from spared axons, or *de novo* axonal growth from spared pathways are likely to improve DIAm function over time. In rats, we have consistently observed ~25% spontaneous recovery in DIAm EMG during eupnoea at 7- and 14-days post C_2SH (Mantilla *et al.*, 2013a;Gransee *et al.*, 2015;Martinez-Galvez *et al.*, 2016;Hernandez-Torres *et al.*, 2017;Sieck *et al.*, 2021;Brown *et al.*, 2022). In concordance, VEH treated rats exhibited ~29% recovery of DIAm EMG during eupnoea by 14-days post C_2SH in our current study. Notably, we have no evidence that “bridging” of the glial scar from injury-side tracts from cranial to the injury to caudal to the injury is a likely cause of spontaneous recovery, with clear lesion demarcation occurring in non-recovered and recovered rats. It is also important to note that the dorsal columns are spared during C_2SH.

A plethora of therapeutic approaches have been shown to improve the proportion of rats with recovered DIAm EMG following C_2SH, including neurotrophic support, intermittent hypoxia and augmentation of glutamatergic or serotonergic receptor activation (Zhou and Goshgarian, 1999;Fuller *et al.*, 2003;Gransee *et al.*, 2013;Mantilla *et al.*, 2013a;Gransee

et al., 2015;Martinez-Galvez *et al.*, 2016;Hernandez-Torres *et al.*, 2017;Wollman *et al.*, 2020;Sieck *et al.*, 2021). Although not all these approaches display even a modicum of the practicality of the daily systemic dosing used in the current study. These previous approaches increase the % of rats recovering to >10% of initial DIAm EMG activity, from ~30% to ~50–80% (Gransee *et al.*, 2013;Mantilla *et al.*, 2013a;Gransee *et al.*, 2015;Martinez-Galvez *et al.*, 2016). Further, these approaches show increased magnitude of DIAm EMG activation compared to initial levels during eupnoea, with enhanced neurotrophic (BDNF/TrkB activation) support improving EMG activity in recovered rats to ~50–90% of initial, compared to the ~25–35% initial activity in spontaneously recovered rats (Gransee *et al.*, 2013;Mantilla *et al.*, 2013a;Gransee *et al.*, 2015;Martinez-Galvez *et al.*, 2016). In the present study, treatment with SPG302 increased the likelihood of recovery following C_2SH ~2.5-fold, compared to VEH treated controls. In addition, treatment with SPG302 significantly increased the magnitude of DIAm RMS EMG at 14-days post C_2SH compared to immediate post-surgery values across all ventilatory behaviours and compared to VEH treated controls at 14-days post C_2SH. Importantly, in recovered SPG302 treated rats, DIAm RMS EMG during eupnoea was ~60% of initial pre-surgery values, compared to ~20% of initial for recovered VEH treated rats. Overall, SPG302 significantly increased the incidence and magnitude of DIAm EMG recovery following C_2SH.

Treatment of C_2SH lesioned rats with SPG302 also provided substantial functional benefits, as evidenced by P_{di} assessment. Following 14 days of SPG302 treatment, SPG302 treated rats had greater P_{di} during eupnoea, HH, occlusion and bilateral phrenic nerve stimulation (P_{dimax}) compared to VEH treated rats. Importantly, the depression in P_{di} during eupnoea, HH and occlusion immediately post-surgery in all VEH and SPG302 treated C_2SH rats compared to SHAM treatment was ameliorated by 14 days of SPG302 treatment. Thus, SPG302 treatment essentially returned ventilatory P_{di} to a pre-surgery level and substantially improved P_{dimax}. A limitation of the current study was that treatment with SPG302 started prior to our 3-day assessment of our C_2SH lesion. Although in the present study we had no activity in any VEH or SPG302 rat at 3 days post C2SH, a few of our prior studies waited until day 3 to commence treatment, thus our improved magnitude of recovery compared to BDNF/TrkB approaches may be a result of earlier more aggressive treatment timing. Notably, none of these outcomes was mediated by any difference in anatomical lesion severity (nor was any evidence of axonal growth “bridging” the glial scar following SPG302 treatment), likely due to our rigorous functional inclusion exclusion/criteria. Similarly, none of the outcomes were influenced unduly by varying degrees of contralateral compensation, with negligeable changes in the DIAm RMS EMG on the contralateral side across differing time points, treatments and behaviours, in staunch agreement with past studies (Martinez-Galvez *et al.*, 2016;Hernandez-Torres *et al.*, 2017).

Although out of the scope of the current study, it is likely that SPG302 treatment improved functional outcomes following C_2SH by enhancing pre- or post-synaptic neurotransmission onto PhMNs. This result was likely achieved by either increasing the number or strength of spared contralateral or latent excitatory synaptic inputs onto PhMNs, or conversely, by increasing the abundance of post-synaptic sites for neural input. Studies of SPG302 in the triple transgenic mouse model of Alzheimer’s disease revealed significant increases in the density of dendritic spines and co-localized pre- and post-synaptic markers (a measure of

functional contacts), but no significant differences in the density of presynaptic markers (Trujillo-Estrada *et al.*, 2021); similar changes have been demonstrated *in vitro*. These observations suggest that SPG302 enhances the formation of postsynaptic elements to which existing presynaptic machinery can fruitfully couple to form a functional synapse. Previous studies using pegylated benzothiazole derivatives, the class of drug to which SPG302 belongs, support these interpretations, with these compounds enhancing F-actin cytoskeleton remodeling (Cifelli *et al.*, 2016;Lee *et al.*, 2016;Zhang *et al.*, 2019;Cifelli *et al.*, 2020). The essential role of F-actin in the maintenance and formation of dendritic spines has been highly characterized (van Bommel *et al.*, 2019;Bucher *et al.*, 2020). Despite motor neurons having lesser spine densities (Bandaru *et al.*, 2015;Fogarty *et al.*, 2016a;Kanjhan *et al.*, 2016;Fogarty *et al.*, 2017a;Fogarty *et al.*, 2017b;2020a;b) compared to other neuronal subtypes (Kawaguchi *et al.*, 2006;Fogarty *et al.*, 2016b;Fogarty *et al.*, 2016c;Klenowski *et al.*, 2017), excitatory dendritic shaft synapses are common in many neurons (and likely motor neurons) (Bourne and Harris, 2011;Fogarty *et al.*, 2013), with similar F-actin mechanisms responsible for generating and maintaining post-synaptic specializations of glutamatergic synapses on dendritic shafts (van Bommel *et al.*, 2019). Alternatively, pre-synaptic F-actin is essential for axon guidance, presynaptic terminal differentiation and the budding of axon collaterals- necessary for creating *de novo* inputs (Zhang and Benson, 2001;Gallo, 2011;Nelson *et al.*, 2013). Thus, while prior evidence favors a post-synaptic locus of SPG302 action, it may enhance the de novo formation of glutamatergic synapses following C_2SH by either a pre- or post-synaptic mechanism. Future investigations will include efforts defining the mode of action of SPG302 in the spinal cord.

Our study did not investigate the pharmacokinetics or timing of treatment with SPG302 in relation to C_2SH, parameters that would inform on the scope of SPG302's potential therapeutic utility in spinal cord injuries. *In vitro* studies have shown spinogenic activity of SPG101 prototypes within an hour, and enhancement of motor function in vivo within 1 week during systemic delivery in a controlled cortical impact rat model of traumatic brain injury (Cifelli *et al.*, 2016;Zhang *et al.*, 2019). Longer term effectiveness out to 1 month was also established this model, and more recently for SPG302 in the triple transgenic mouse model of Alzheimer disease (Trujillo-Estrada *et al.*, 2021). Of clinical relevance, it remains to be determined whether SPG302 will elicit any improvement in chronically non-recovered rats following C_2SH, where BDNF/TrkB approaches have had some success (Sieck *et al.*, 2021). It remains unknown whether SPG302 will be effective in models that more closely approximate human spinal cord injuries, where frank PhMN death and a robust inflammatory response are prevalent as modelled by the C_4 hemi-contusion (Alvarez-Argote *et al.*, 2016;Fogarty and Sieck, 2020).

In summary, this study provides two major advances in C_2SH investigation that are highly informative to the field. Firstly, we characterize a suite of EMG and functional deficits across a variety of behaviours following C_2SH. Secondly, we exhibit exciting preclinical evidence for improved outcomes in C_2SH by treatment with a novel synaptic regenerative therapeutic, SPG302. This promising therapeutic approach could lead to new opportunities in a space with a dearth of pharmacological or translatable discoveries.

Acknowledgements:

We thank Rebecca Macken, Yun-Hua Fang and Dr. Obaid U. Khurram for their assistance in this project.

Funding:

This research was funded by NIH grant HLBI R01-146114

Biography

Matt is currently an assistant professor at Mayo Clinic, Minnesota, arriving as a postdoctoral NHMRC Fellow in 2016 following his BVSc (2008) and PhD (2014) at The University of Queensland, Australia. He is striving to establish an independent research niche exploring and ameliorating ageing and neurodegeneration associated motor defects. His published oeuvre comprises all the station-stops between the motor cortex and skeletal muscle fibres, during conditions such as development, injury, ageing and disease. Most of Matt's career has involved identifying pathogenetic dysfunctions. This therapeutic investigation marks a pleasant change of theme. To date, he has never performed a Western Blot.

Data Availability:

All individual data are presented in the Results, Figures and Tables.

REFERENCES

Alvarez-Argote S, Gransee HM, Mora JC, Stowe JM, Jorgenson AJ, Sieck GC, and Mantilla CB (2016). The Impact of Midcervical Contusion Injury on Diaphragm Muscle Function. J Neurotrauma 33, 500–509. [PubMed: 26413840]

Aubier M, Murciano D, Lecocguic Y, Viires N, and Pariente R (1985). Bilateral phrenic stimulation: a simple technique to assess diaphragmatic fatigue in humans. J Appl Physiol (1985) 58, 58–64. [PubMed: 3968023]

Bandaru SP, Liu S, Waxman SG, and Tan AM (2015). Dendritic spine dysgenesis contributes to hyperreflexia after spinal cord injury. J Neurophysiol 113, 1598–1615. [PubMed: 25505110]

Bellemare F, and Bigland-Ritchie B (1984). Assessment of human diaphragm strength and activation using phrenic nerve stimulation. Respir Physiol 58, 263–277. [PubMed: 6528104]

Bellemare F, Bigland-Ritchie B, and Woods JJ (1986). Contractile properties of the human diaphragm in vivo. J Appl Physiol 61, 1153–1161. [PubMed: 3759756]

Beth Zimmer M, Grant JS, Ayar AE, and Goshgarian HG (2015). Ipsilateral inspiratory intercostal muscle activity after C2 spinal cord hemisection in rats. J Spinal Cord Med 38, 224–230. [PubMed: 24969369]

Bourne JN, and Harris KM (2011). Coordination of size and number of excitatory and inhibitory synapses results in a balanced structural plasticity along mature hippocampal CA1 dendrites during LTP. Hippocampus 21, 354–373. [PubMed: 20101601]

Brandenburg JE, Fogarty MJ, Brown AD, and Sieck GC (2020). Phrenic motor neuron loss in an animal model of early onset hypertonia. J Neurophysiol 123, 1682–1690. [PubMed: 32233911]

Brown AD, Fogarty MJ, Davis LA, Dasgupta D, Mantilla CB, and Sieck GC (2022). Mitochondrial Adaptations to Inactivity in Diaphragm Muscle Fibers. J Appl Physiol (1985).

Bucher M, Fanutza T, and Mikhaylova M (2020). Cytoskeletal makeup of the synapse: Shaft versus spine. Cytoskeleton (Hoboken) 77, 55–64. [PubMed: 31762205]

Cifelli JL, Berg KR, and Yang J (2020). Benzothiazole amphiphiles promote RasGRF1-associated dendritic spine formation in human stem cell-derived neurons. FEBS Open Bio 10, 386–395.

Cifelli JL, Dozier L, Chung TS, Patrick GN, and Yang J (2016). Benzothiazole Amphiphiles Promote the Formation of Dendritic Spines in Primary Hippocampal Neurons. J Biol Chem 291, 11981–11992. [PubMed: 27022020]

Denton M, and Mckinlay J (2009). Cervical cord injury and critical care. Continuing Education in Anaesthesia Critical Care & Pain 9, 82–86.

Elmallah MK, Pagliardini S, Turner SM, Cerreta AJ, Falk DJ, Byrne BJ, Greer JJ, and Fuller DD (2015). Stimulation of Respiratory Motor Output and Ventilation in a Murine Model of Pompe Disease by Ampakines. Am J Respir Cell Mol Biol 53, 326–335. [PubMed: 25569118]

Fogarty MJ, Brandenburg JE, Zhan WZ, and Sieck GC (2022). Diaphragm Muscle Function in a Mouse Model of Early Onset Spasticity. J Appl Physiol (1985).

Fogarty MJ, Hammond LA, Kanjhan R, Bellingham MC, and Noakes PG (2013). A method for the three-dimensional reconstruction of Neurobiotin-filled neurons and the location of their synaptic inputs. Front Neural Circuits 7, 153. [PubMed: 24101895]

Fogarty MJ, Kanjhan R, Bellingham MC, and Noakes PG (2016a). Glycinergic Neurotransmission: A Potent Regulator of Embryonic Motor Neuron Dendritic Morphology and Synaptic Plasticity. J Neurosci 36, 80–87. [PubMed: 26740651]

Fogarty MJ, Kanjhan R, Yanagawa Y, Noakes PG, and Bellingham MC (2017a). Alterations in hypoglossal motor neurons due to GAD67 and VGAT deficiency in mice. Exp Neurol 289, 117–127. [PubMed: 27956032]

Fogarty MJ, Klenowski PM, Lee JD, Drieberg-Thompson JR, Bartlett SE, Ngo ST, Hilliard MA, Bellingham MC, and Noakes PG (2016b). Cortical synaptic and dendritic spine abnormalities in a presymptomatic TDP-43 model of amyotrophic lateral sclerosis. Sci Rep 6, 37968. [PubMed: 27897242]

Fogarty MJ, Mantilla CB, and Sieck GC (2018a). Breathing: Motor Control of Diaphragm Muscle. Physiology (Bethesda) 33, 113–126. [PubMed: 29412056]

Fogarty MJ, Mu EW, Noakes PG, Lavidis NA, and Bellingham MC (2016c). Marked changes in dendritic structure and spine density precede significant neuronal death in vulnerable cortical pyramidal neuron populations in the SOD1(G93A) mouse model of amyotrophic lateral sclerosis. Acta Neuropathol Commun 4, 77. [PubMed: 27488828]

Fogarty MJ, Mu EWH, Lavidis NA, Noakes PG, and Bellingham MC (2017b). Motor Areas Show Altered Dendritic Structure in an Amyotrophic Lateral Sclerosis Mouse Model. Front Neurosci 11, 609. [PubMed: 29163013]

Fogarty MJ, Mu EWH, Lavidis NA, Noakes PG, and Bellingham MC (2020a). Size-dependent dendritic maladaptations of hypoglossal motor neurons in SOD1(G93A) mice. Anat Rec (Hoboken).

Fogarty MJ, Mu EWH, Lavidis NA, Noakes PG, and Bellingham MC (2020b). Size-Dependent Vulnerability of Lumbar Motor Neuron Dendritic Degeneration in SOD1(G93A) Mice. Anat Rec (Hoboken) 303, 1455–1471. [PubMed: 31509351]

Fogarty MJ, Omar TS, Zhan WZ, Mantilla CB, and Sieck GC (2018b). Phrenic Motor Neuron Loss in Aged Rats. J Neurophysiol 119, 1852–1862. [PubMed: 29412773]

Fogarty MJ, and Sieck GC (2019). Evolution and Functional Differentiation of the Diaphragm Muscle of Mammals. Compr Physiol 9, 715–766. [PubMed: 30873594]

Fogarty MJ, and Sieck GC (2020). Spinal cord injury and diaphragm neuromotor control. Expert Rev Respir Med, 1–12.

Fuller DD, Doperalski NJ, Dougherty BJ, Sandhu MS, Bolser DC, and Reier PJ (2008). Modest spontaneous recovery of ventilation following chronic high cervical hemisection in rats. Exp Neurol 211, 97–106. [PubMed: 18308305]

Fuller DD, Golder FJ, Olson EB Jr., and Mitchell GS (2006). Recovery of phrenic activity and ventilation after cervical spinal hemisection in rats. J Appl Physiol 100, 800–806. [PubMed: 16269524]

Fuller DD, Johnson SM, Olson EB Jr., and Mitchell GS (2003). Synaptic pathways to phrenic motoneurons are enhanced by chronic intermittent hypoxia after cervical spinal cord injury. J Neurosci 23, 2993–3000. [PubMed: 12684486]

Gallo G (2011). The cytoskeletal and signaling mechanisms of axon collateral branching. Dev Neurobiol 71, 201–220. [PubMed: 21308993]

Geiger PC, Cody MJ, Macken RL, and Sieck GC (2000). Maximum specific force depends on myosin heavy chain content in rat diaphragm muscle fibers. J Appl Physiol 89, 695–703. [PubMed: 10926656]

Gill LC, Mantilla CB, and Sieck GC (2015). Impact of unilateral denervation on transdiaphragmatic pressure. Respir Physiol Neurobiol 210, 14–21. [PubMed: 25641347]

Golder FJ, Fuller DD, Davenport PW, Johnson RD, Reier PJ, and Bolser DC (2003). Respiratory motor recovery after unilateral spinal cord injury: eliminating crossed phrenic activity decreases tidal volume and increases contralateral respiratory motor output. J Neurosci 23, 2494–2501. [PubMed: 12657710]

Goshgarian HG, Ellenberger HH, and Feldman JL (1991). Decussation of bulbospinal respiratory axons at the level of the phrenic nuclei: a possible substrate for the crossed-phrenic phenomenon. Exp Neurol 111, 135–139. [PubMed: 1984430]

Gransee HM, Gonzalez Porras MA, Zhan WZ, Sieck GC, and Mantilla CB (2017). Motoneuron glutamatergic receptor expression following recovery from cervical spinal hemisection. J Comp Neurol 525, 1192–1205. [PubMed: 27650492]

Gransee HM, Zhan WZ, Sieck GC, and Mantilla CB (2013). Targeted Delivery of TrkB Receptor to Phrenic Motoneurons Enhances Functional Recovery of Rhythmic Phrenic Activity after Cervical Spinal Hemisection. PLoS One 8, e64755. [PubMed: 23724091]

Gransee HM, Zhan WZ, Sieck GC, and Mantilla CB (2015). Localized Delivery of Brain-Derived Neurotrophic Factor-Expressing Mesenchymal Stem Cells Enhances Functional Recovery following Cervical Spinal Cord Injury. J Neurotrauma 32, 185–193. [PubMed: 25093762]

Grundy D (2015). Principles and standards for reporting animal experiments in The Journal of Physiology and Experimental Physiology. J Physiol 593, 2547–2549. [PubMed: 26095019]

Hadley SD, Walker PD, and Goshgarian HG (1999). Effects of serotonin inhibition on neuronal and astrocyte plasticity in the phrenic nucleus 4 h following C2 spinal cord hemisection. Exp Neurol 160, 433–445. [PubMed: 10619560]

Hernandez-Torres V, Gransee HM, Mantilla CB, Wang Y, Zhan WZ, and Sieck GC (2017). BDNF effects on functional recovery across motor behaviors after cervical spinal cord injury. J Neurophysiol 117, 537–544. [PubMed: 27832605]

Kanjhan R, Fogarty MJ, Noakes PG, and Bellingham MC (2016). Developmental changes in the morphology of mouse hypoglossal motor neurons. Brain Struct Funct 221, 3755–3786. [PubMed: 26476929]

Kawaguchi Y, Karube F, and Kubota Y (2006). Dendritic branch typing and spine expression patterns in cortical nonpyramidal cells. Cereb Cortex 16, 696–711. [PubMed: 16107588]

Kennedy MB (1997). The postsynaptic density at glutamatergic synapses. Trends Neurosci 20, 264–268. [PubMed: 9185308]

Khurram OU, Fogarty MJ, Rana S, Vang P, Sieck GC, and Mantilla CB (2019). Diaphragm muscle function following midcervical contusion injury in rats. J Appl Physiol (1985) 126, 221–230. [PubMed: 30236045]

Khurram OU, Fogarty MJ, Sarrafian TL, Bhatt A, Mantilla CB, and Sieck GC (2018). Impact of aging on diaphragm muscle function in male and female Fischer 344 rats. Physiol Rep 6, e13786. [PubMed: 29981218]

Klenowski PM, Wright SE, Mu EWH, Noakes PG, Lavidis NA, Bartlett SE, Bellingham MC, and Fogarty MJ (2017). Investigating Methodological Differences in the Assessment of Dendritic Morphology of Basolateral Amygdala Principal Neurons-A Comparison of Golgi-Cox and Neurobiotin Electroporation Techniques. Brain Sci 7.

Lee NJ, Song JM, Cho HJ, Sung YM, Lee T, Chung A, Hong SH, Cifelli JL, Rubinshtein M, Habib LK, Capule CC, Turner RS, Pak DT, Yang J, and Hoe HS (2016). Hexa (ethylene glycol)

derivative of benzothiazole aniline promotes dendritic spine formation through the RasGRF1-Ras dependent pathway. Biochim Biophys Acta 1862, 284–295. [PubMed: 26675527]

Lipski J, Zhang X, Kruszewska B, and Kanjhan R (1994). Morphological study of long axonal projections of ventral medullary inspiratory neurons in the rat. Brain Res 640, 171–184. [PubMed: 8004446]

Mantilla CB, Bailey JP, Zhan WZ, and Sieck GC (2012). Phrenic motoneuron expression of serotonergic and glutamatergic receptors following upper cervical spinal cord injury. Exp Neurol 234, 191–199. [PubMed: 22227062]

Mantilla CB, Gransee HM, Zhan WZ, and Sieck GC (2013a). Motoneuron BDNF/TrkB signaling enhances functional recovery after cervical spinal cord injury. Exp Neurol 247C, 101–109.

Mantilla CB, Greising SM, Zhan WZ, Seven YB, and Sieck GC (2013b). Prolonged C2 spinal hemisection-induced inactivity reduces diaphragm muscle specific force with modest, selective atrophy of type IIx and/or IIb fibers. J Appl Physiol 114, 380–386. [PubMed: 23195635]

Mantilla CB, Seven YB, Hurtado-Palomino JN, Zhan WZ, and Sieck GC (2011). Chronic assessment of diaphragm muscle EMG activity across motor behaviors. Respir Physiol Neurobiol 177, 176–182. [PubMed: 21414423]

Martinez-Galvez G, Zambrano JM, Diaz Soto JC, Zhan WZ, Gransee HM, Sieck GC, and Mantilla CB (2016). TrkB gene therapy by adeno-associated virus enhances recovery after cervical spinal cord injury. Exp Neurol 276, 31–40. [PubMed: 26607912]

Mccrimmon DR, Dekin MS, and Mitchell GS (1995). “Glutamate, GABA, and serotonin in ventilatory control.,” in Regulation of Breathing, eds. Dempsey JA & Pack AL. Second ed (New York: Marcel Dekker Inc.), 151–218.

Mccrimmon DR, Smith JC, and Feldman JL (1989). Involvement of excitatory amino acids in neurotransmission of inspiratory drive to spinal respiratory motoneurons. J Neurosci 9, 1910–1921. [PubMed: 2542482]

Miyata H, Zhan WZ, Prakash YS, and Sieck GC (1995). Myoneural interactions affect diaphragm muscle adaptations to inactivity. J Appl Physiol 79, 1640–1649. [PubMed: 8594024]

Moreno DE, Yu XJ, and Goshgarian HG (1992). Identification of the axon pathways which mediate functional recovery of a paralyzed hemidiaphragm following spinal cord hemisection in the adult rat. Exp Neurol 116, 219–228. [PubMed: 1375167]

Nelson JC, Stavoe AK, and Colon-Ramos DA (2013). The actin cytoskeleton in presynaptic assembly. Cell Adh Migr 7, 379–387. [PubMed: 23628914]

Paterson G (1965). Twitch responses with acetylcholine in the isolated innervated and chronically denervated rat diaphragms and their modification by neuromuscular blocking agents. J Pharm Pharmacol 17, 281–294. [PubMed: 4378670]

Porter J (1895). The path of the respiratory impulse from the bulb to the phrenic nuclei. J Physiol (Lond) 17, 455–485.

Prakash YS, Miyata H, Zhan WZ, and Sieck GC (1999). Inactivity-induced remodeling of neuromuscular junctions in rat diaphragmatic muscle. Muscle Nerve 22, 307–319. [PubMed: 10086891]

Rana S, Sieck GC, and Mantilla CB (2020a). Heterogeneous glutamatergic receptor mRNA expression across phrenic motor neurons in rats. J Neurochem 153, 586–598. [PubMed: 31563147]

Rana S, Zhan WZ, Mantilla CB, and Sieck GC (2020b). Disproportionate loss of excitatory inputs to smaller phrenic motor neurons following cervical spinal hemisection. J Physiol.

Sieck GC, and Fournier M (1989). Diaphragm motor unit recruitment during ventilatory and nonventilatory behaviors. J Appl Physiol 66, 2539–2545. [PubMed: 2745316]

Sieck GC, Gransee HM, Zhan WZ, and Mantilla CB (2021). Acute intrathecal BDNF enhances functional recovery after cervical spinal cord injury in rats. J Neurophysiol 125, 2158–2165. [PubMed: 33949892]

Singh LP, Devi TS, and Nantwi KD (2012). Theophylline regulates inflammatory and neurotrophic factor signals in functional recovery after C2-hemisection in adult rats. Exp Neurol 238, 79–88. [PubMed: 22981449]

Streeter KA, Sunshine MD, Patel S, Gonzalez-Rothi EJ, Reier PJ, Baekey DM, and Fuller DD (2017). Intermittent Hypoxia Enhances Functional Connectivity of Midcervical Spinal Interneurons. J Neurosci 37, 8349–8362. [PubMed: 28751456]

Streeter KA, Sunshine MD, Patel SR, Gonzalez-Rothi EJ, Reier PJ, Baekey DM, and Fuller DD (2020). Mid-cervical interneuron networks following high cervical spinal cord injury. Respir Physiol Neurobiol 271, 103305. [PubMed: 31553921]

Sunshine MD, Sutor TW, Fox EJ, and Fuller DD (2020). Targeted activation of spinal respiratory neural circuits. Exp Neurol 328, 113256. [PubMed: 32087253]

Tai Q, and Goshgarian HG (1996). Ultrastructural quantitative analysis of glutamatergic and GABAergic synaptic terminals in the phrenic nucleus after spinal cord injury. J Comp Neurol 372, 343–355. [PubMed: 8873865]

Trelease RB, Sieck GC, and Harper RM (1982). A new technique for acute and chronic recording of crural diaphragm EMG in cats. Electroencephalogr Clin Neurophysiol 53, 459–462. [PubMed: 6175508]

Trujillo-Estrada L, Vanderklish PW, Nguyen MMT, Kuang RR, Nguyen C, Huynh E, Da Cunha C, Javonillo DI, Forner S, Martini AC, Sarraf ST, Simmon VF, Baglietto-Vargas D, and Laferla FM (2021). SPG302 Reverses Synaptic and Cognitive Deficits Without Altering Amyloid or Tau Pathology in a Transgenic Model of Alzheimer's Disease. Neurotherapeutics 18, 2468–2483. [PubMed: 34738197]

Van Bommel B, Konietzny A, Kobler O, Bar J, and Mikhaylova M (2019). F-actin patches associated with glutamatergic synapses control positioning of dendritic lysosomes. EMBO J 38, e101183. [PubMed: 31267565]

Warren PM, Steiger SC, Dick TE, Macfarlane PM, Alilain WJ, and Silver J (2018). Rapid and robust restoration of breathing long after spinal cord injury. Nat Commun 9, 4843. [PubMed: 30482901]

Watson C, Paxinos G, Kayalioglu G, and Heise C (2009). "Chapter 15 - Atlas of the Rat Spinal Cord," in The Spinal Cord A Christopher and Dana Reeve Foundation Text and Atlas, eds. Watson C, Paxinos G & Kayalioglu G. Academic Press), 238–306.

Wollman LB, Streeter KA, Fusco AF, Gonzalez-Rothi EJ, Sandhu MS, Greer JJ, and Fuller DD (2020). Ampakines stimulate phrenic motor output after cervical spinal cord injury. Exp Neurol 334, 113465. [PubMed: 32949571]

Zhang W, and Benson DL (2001). Stages of synapse development defined by dependence on Factin. J Neurosci 21, 5169–5181. [PubMed: 11438592]

Zhang Y, Chopp M, Rex CS, Simmon VF, Sarraf ST, Zhang ZG, Mahmood A, and Xiong Y (2019). A Small Molecule Spinogenic Compound Enhances Functional Outcome and Dendritic Spine Plasticity in a Rat Model of Traumatic Brain Injury. J Neurotrauma 36, 589–600. [PubMed: 30014757]

Zhou SY, and Goshgarian HG (1999). Effects of serotonin on crossed phrenic nerve activity in cervical spinal cord hemisected rats. Exp Neurol 160, 446–453. [PubMed: 10619561]

Key Points:

Despite advances in our understanding of the effects of cervical hemisection (C_2SH) on diaphragm muscle (DIAm,) EMG activity, very little is understood about the impact of C_2SH on the gamut of ventilatory and non-ventilatory transdiaphragmatic pressures (P_{di}).

Recovery of DIAm activity following C_2SH is improved using a variety of approaches, but very few pharmaceuticals have been shown to be effective. One way of improving DIAm recovery is to enhance the amount of latent local spared connections onto phrenic motor neurons. A novel pegylated benzothiazole derivatives enhances synaptogenesis in a variety of neurodegenerative conditions.

Here, using a novel therapeutic SPG302, we show that 14 days of treatment with SPG302 ameliorated DIAm EMG and P_{di} deficits compared to vehicle controls.

Our results show that SPG302 is a compound with a very promising potential for use in improving functional outcomes post spinal cord injury.

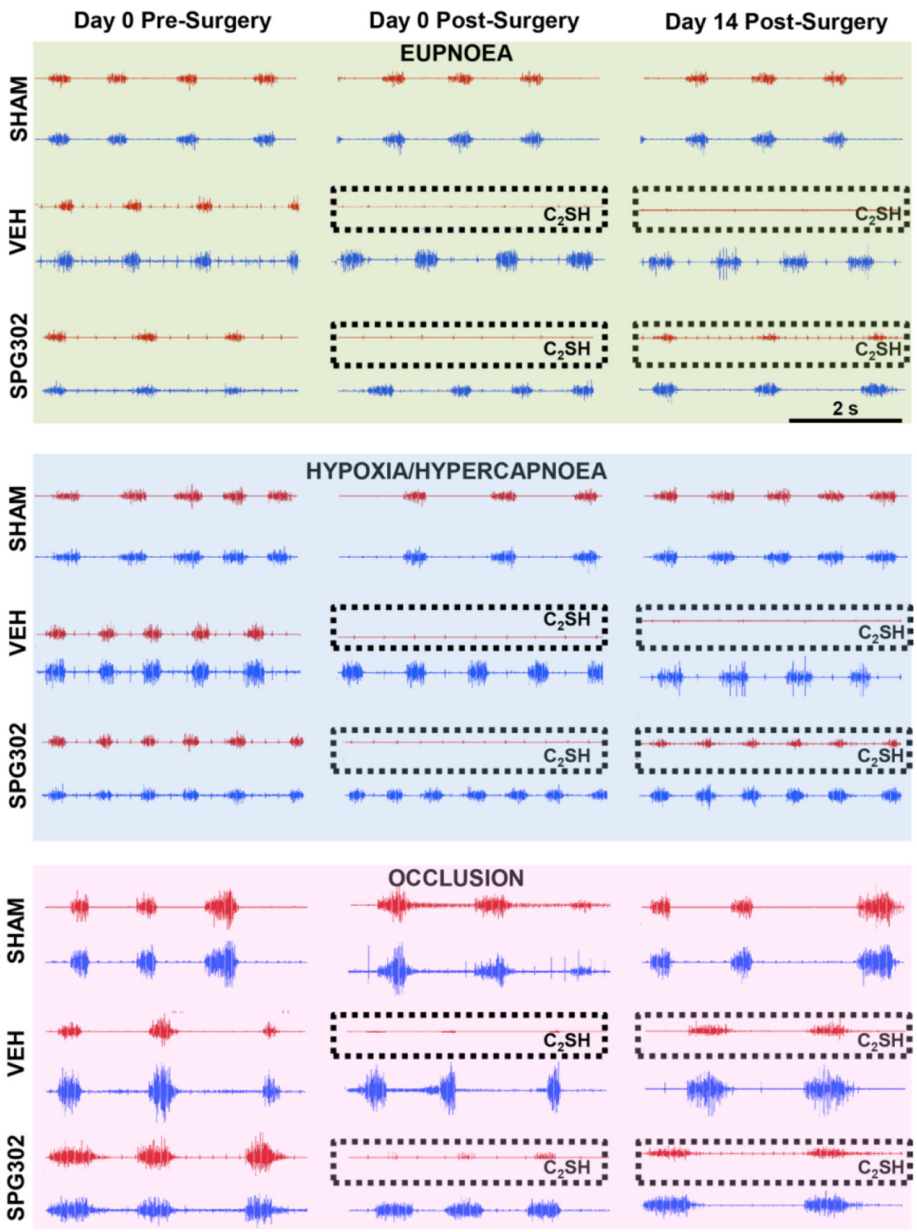

Figure 1.

Representative recordings of right (red) and left (blue) DIAm EMG activity from a rats that underwent sham surgery (SHAM) or C_2SH surgery (right side, dotted rectangles) and were subsequently treated with DMSO vehicle (VEH) or SPG302. Recordings across all behaviours were obtained immediately before laminectomy (pre-surgery) on day 0, immediately after C_2SH on day 0 or laminectomy in sham controls (post-surgery) and 14 days after surgery.

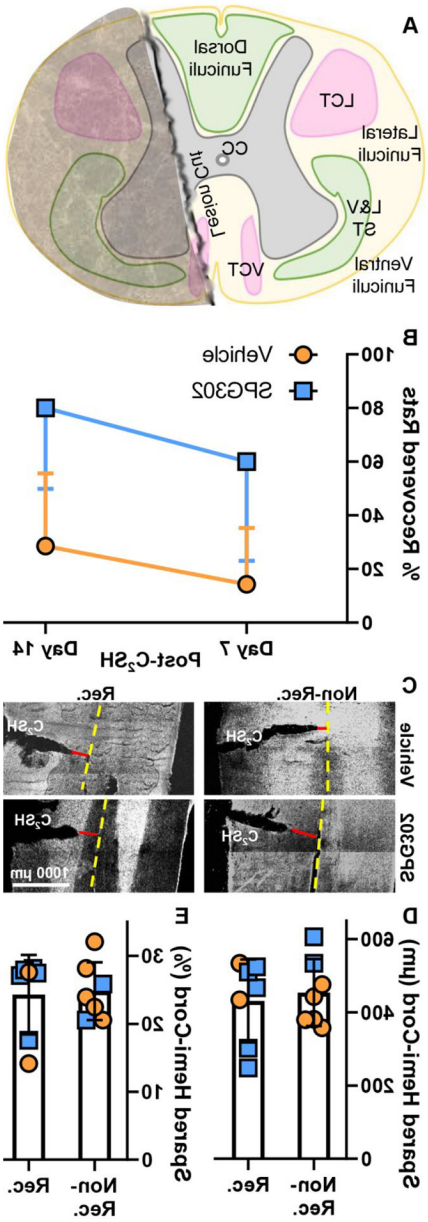

Figure 2:

A: Schematic of the C_2SH lesion employed in the present study, note the severing of the lateral and ventral funiculi, and the preservation of the dorsal funiculus and some sparing adjacent to the central canal (CC). Descending motor tracts (magenta) comprising the lateral and ventral coticospinal tracts (LCT and VCT) along with ascending sensory (green) lateral and ventral spinothalamic tracts (L&VST) are depicted as lesioned (grey semitransparency) on the right hand side. **B:** The % (mean ± SD) of rats that recovered (> 10% initial RMS DIAm EMG during eupnoea) was greater in SPG302 treated rats (blue squares) compared to VEH rats (orange circles) at 7- (P=0.032) and 14-days post-C_2SH (P=0.036; n=14 VEH, n=10 SPG302; Fisher's exact test). **C:** Epifluorescence images of spinal cord histology of horizontal sections (70 µm) at the level of the central canal (yellow dashed

line) in non-revovered (Non-Rec.) and recovered (Rec.) vehicle and SPG302 treated rats. The quantification of the spared region following right sided C_2SH is illustrated by the red line. **D:** Scatterplot shows the spared portion (from the central canal to the cut lesion edge) of the spinal cord at the middle "equatorial" latitude of the C_2 spinal cord being unchanged between non-recovered (n=7) and recovered rats (n=7; P=0.687, Student's unpaired t-test), regardless of treatment with VEH (orange circles) or SPG302 (blue squares). **E:** Scatterplot shows the spared portion expressed as a % of the radius at the middle "equatorial" latitude of C_2 being unchanged between non-recovered (n=7) and recovered rats (n=7; P=0.855, Student's unpaired t-test), regardless of treatment with VEH (orange circles) or SPG302 (blue squares).

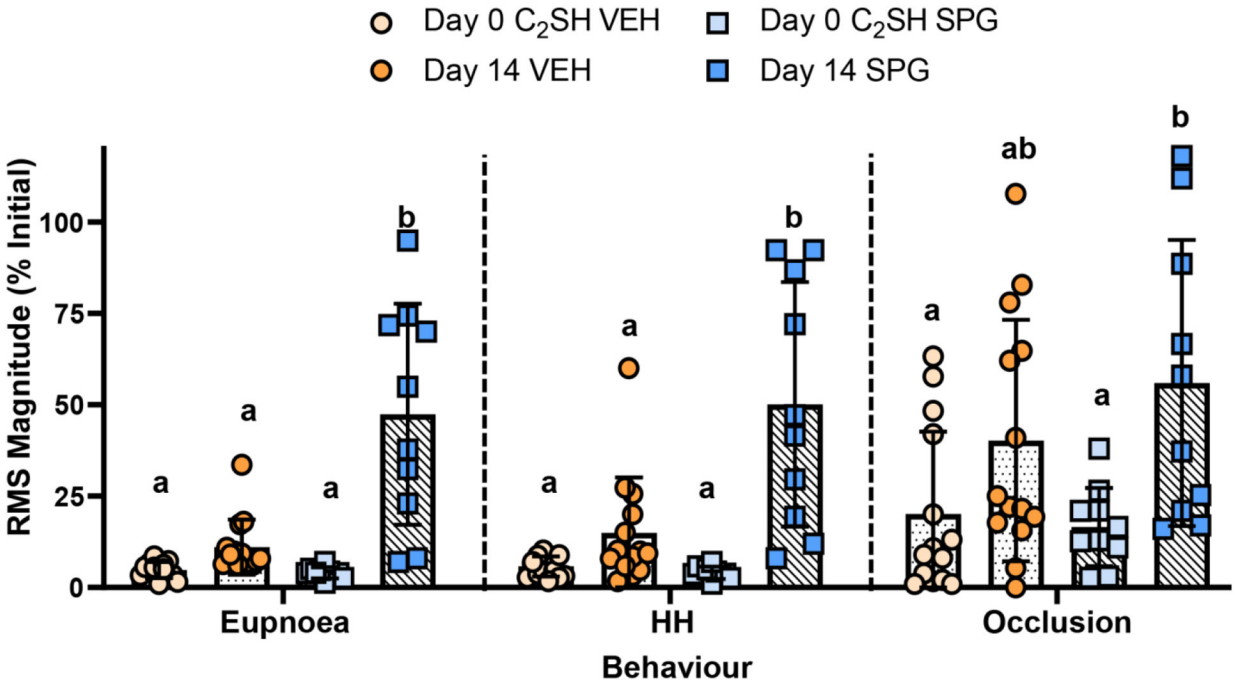

Figure 3.

DIAm RMS EMG activity was calculated for each animal and behaviour and normalized to the corresponding day 0 pre-surgery mean DIAm RMS EMG (i.e., 100 is the starting point for eupnoea, HH and occlusion within each rat). The scatterplot shows mean DIAm RMS EMG for the right injured side for all behaviours with mean (± SD) values of each VEH (orange circle symbols) or SPG302 treated (blue square symbols) rats represented by each dotpoint. Within each behaviour, different levels of DIAm RMS EMG activity are indicated by different letters (ie., a ≠ b ≠ c, with $P<0.05$). Immediately following C_2SH, DIAm RMS EMG activity was reduced to <10% of initial during eupnoea and HH and <20% of initial during occlusion in both VEH and SPG302 treated rats. In VEH rats, 14-days post-C_2SH (darkened symbols) did not improve DIAm RMS EMG in eupnoea or HH ($P>0.05$) compared to immediate post-C_2SH values. However, there was an increase at 14-days following C2SH in the occlusion DIAm RMS EMG compared to immediately post-C_2SH ($P<0.05$). Treatment with SPG302 improved the magnitude of DIAm RMS EMG at 14 days following C_2SH (darkened symbols) in all behaviours. DIAm RMS EMG activity was returned to ~50% of initial values in SPG302 rats during eupnoea, HH and occlusion ($P<0.05$ in all comparisons). In addition, compared immediately post C_2SH, 14-day treatment with SPG302 led to greater DIAm RMS EMG compared to 14-day VEH rats during eupnoea and HH ($P<0.05$). Three-way ANOVA with Bonferroni post-test, $n=14$ VEH, $n=10$ SPG302.

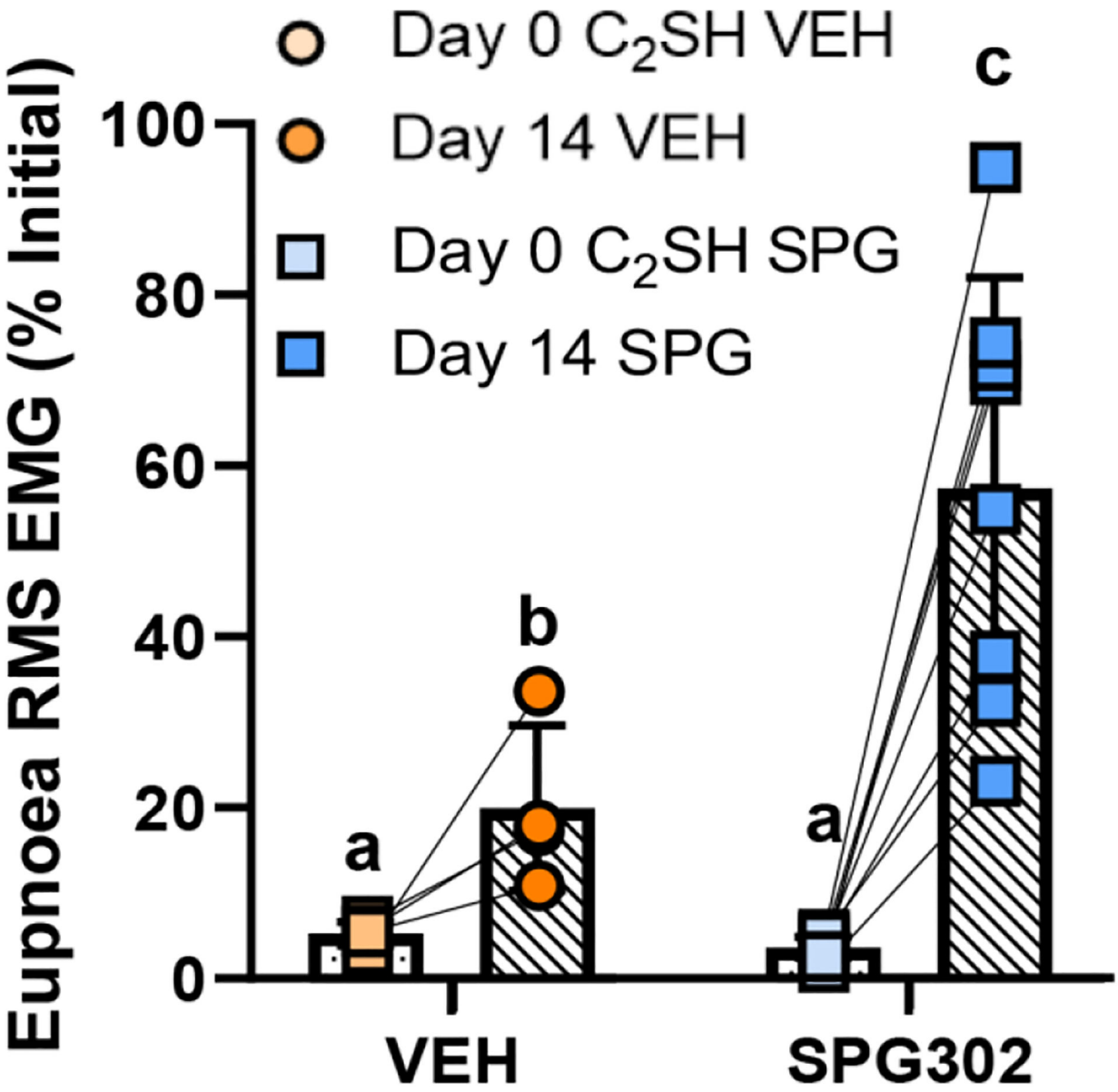

Figure 4.

In exclusively recovered rats (ie., those that exhibited >10% of initial DIAm RMS EMG druring eupnoea) at 14 days following C_2SH, DIAm RMS EMG (mean ± SD) was greater in SPG302 treated (blue squares), compared to VEH rats (orange circles). Different letters indicate significant differences ($P<0.05$). Two-way ANOVA with Bonferroni post-test, $n=4$ VEH, $n=8$ SPG302.

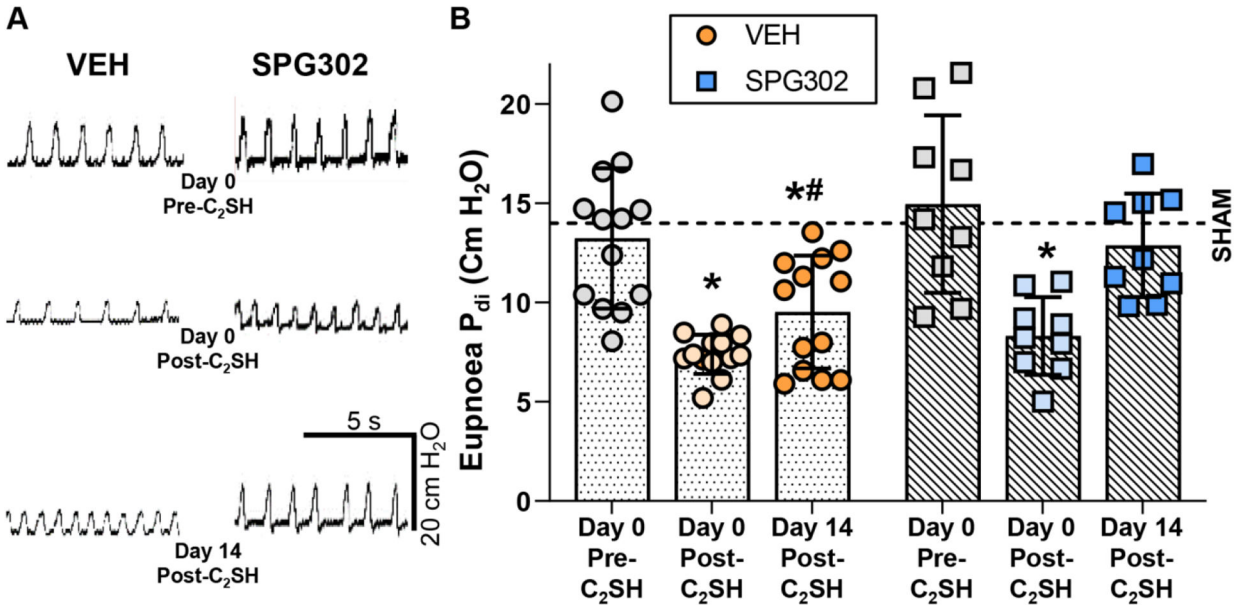

Figure 5.

A: Example P_{di} traces during eupnoea immediately prior to surgery (day 0), immediately following C_2SH (day 0) and 14-days after C_2SH in VEH and SPG302 rats. **B:** Scatterplot of P_{di} (mean ± SD), (with SHAM values represented by a dashed line) illustrate a marked reduction in P_{di} during eupnoea immediately following C_2SH in VEH (light orange circles) and SPG302 (light blue squares) treated rats compard to pre-surgery (grey symbols; *, $P<0.05$). By 14-days following C_2SH, VEH treated rats (dark orange circles) continue to have reduced P_{di} during eupnoea compared to SHAM (and pre-injury) (*, $P<0.05$) and to SPG302 treated rats (dark blue squares; $^{\#}$, $P<0.05$). Furthermore, P_{di} during eupnoea in SPG302 treated rats has returned to SHAM (and pre-injury) levels by day 14. Two-way ANOVA with Bonferroni post-test, $n=7$ SHAM, $n=13$ VEH, $n=9$ SPG302.

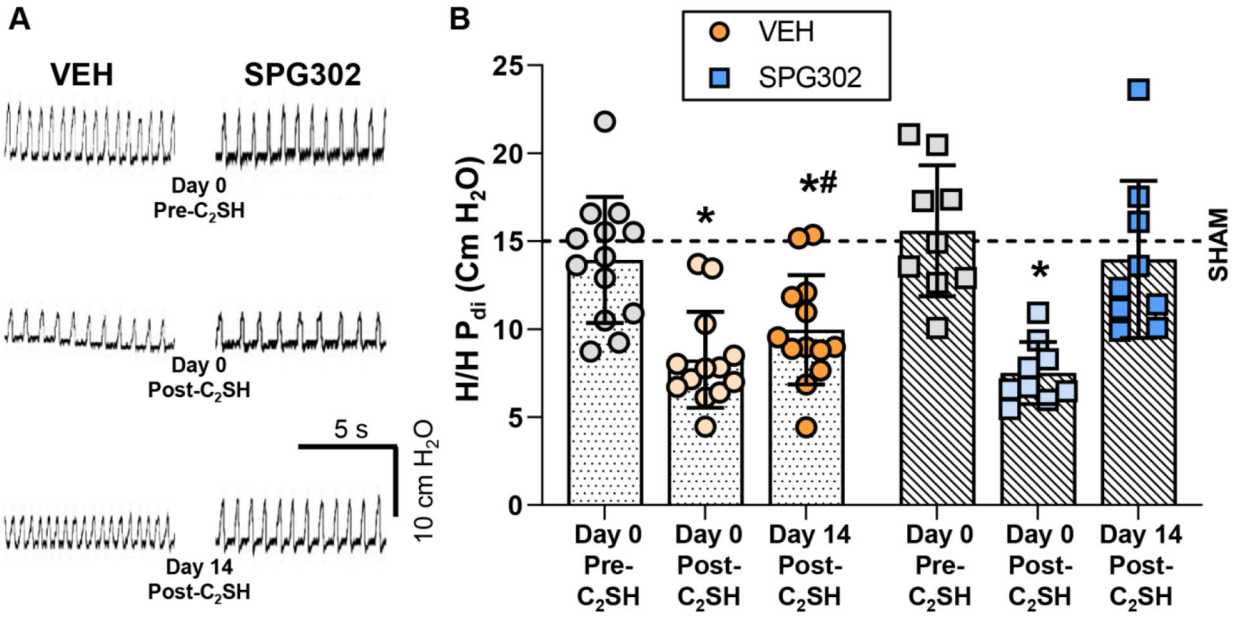

Figure 6.

A: Example P_{di} traces during HH immediately prior to surgery (day 0), immediately following C_2SH (day 0) and 14-days after C_2SH in VEH and SPG302 rats. **B:** Scatterplot of P_{di} (mean ± SD), (with SHAM values represented by a dashed line) illustrate a marked reduction in P_{di} during HH immediately following C_2SH in VEH (light orange circles) and SPG302 treated rats (light blue squares) compard to pre-surgery (grey symbols; *, $P<0.05$). By 14-days following C_2SH, VEH treated rats (dark orange circles) continue to have reduced P_{di} during HH compared to SHAM (and pre-injury) (*, $P<0.05$) and to SPG302 treated rats (dark blue squares; $^{\#}$, $P<0.05$). Furthermore, P_{di} during HH in SPG302 treated rats has returned to SHAM (and pre-injury) levels by day 14. Two-way ANOVA with Bonferroni post-test, $n=7$ SHAM, $n=13$ VEH, $n=9$ SPG302.

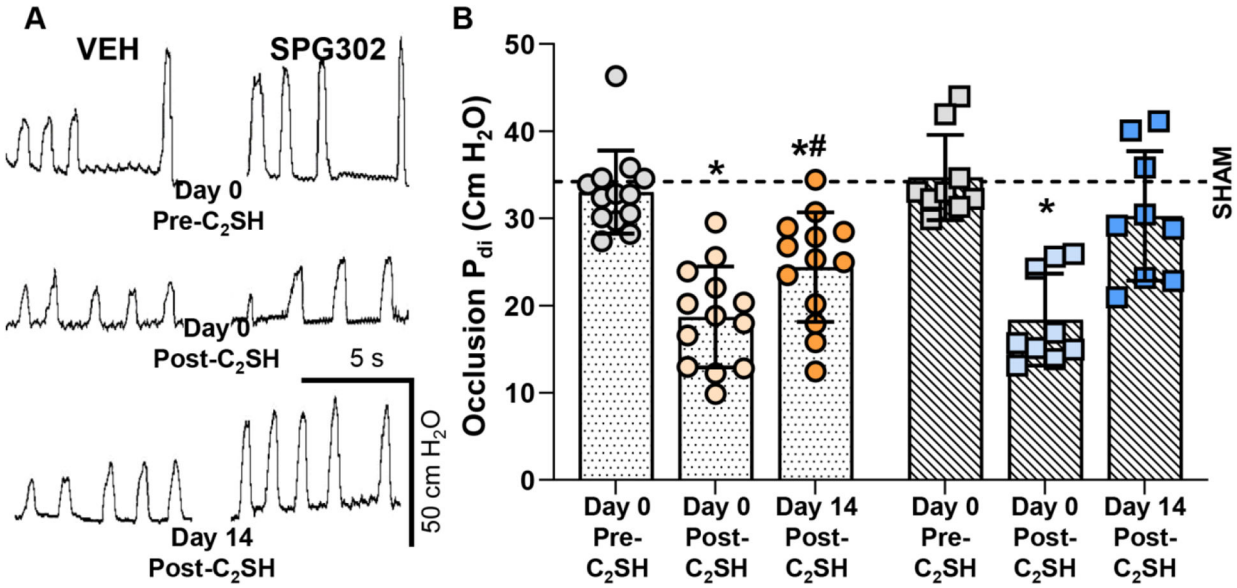

Figure 7.

A: Example P_{di} traces during occlusion immediately prior to surgery (day 0), immediately following C_2SH (day 0) and 14-days after C_2SH in VEH and SPG302 rats. **B:** Scatterplot of P_{di} (mean ± SD), (with SHAM values represented by a dashed line) illustrate a marked reduction in P_{di} during occlusion immediately following C_2SH in VEH (light orange circle) and SPG302 treated rats (light blue squares) compared to presurgery values (grey symbols; *, $P<0.05$). By 14-days following C_2SH, VEH treated rats (dark orange circles) continue to have reduced P_{di} during occlusion compared to SHAM (and pre-injury) (*, $P<0.05$) and to SPG302 treated rats (dark blue squares; $^{\#}$, $P<0.05$). Furthermore, P_{di} during occlusion in SPG302 treated rats has returned to SHAM (and pre-injury) levels by day 14. Two-way ANOVA with Bonferroni post-test, $n=7$ SHAM, $n=13$ VEH, $n=9$ SPG302.

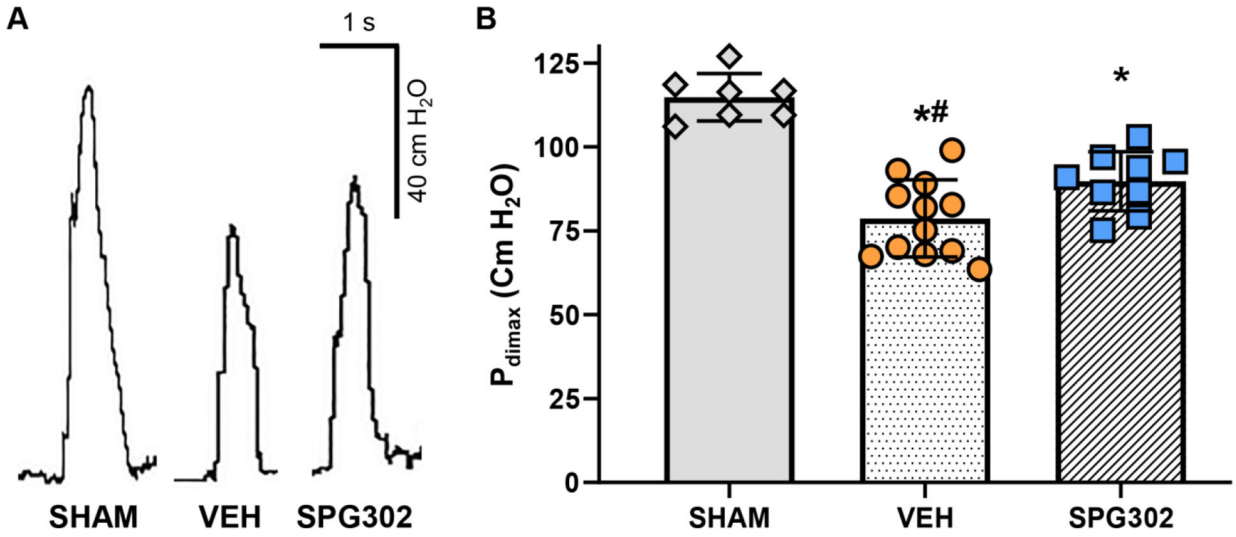

Figure 8.

A: Example P_{dimax} traces (achieved via bilaterl phrenic nerve stimulation) at terminal experiments (day 14) in SHAM, VEH and SPG302 rats. **B:** Scatterplot of P_{dimax} (mean ± SD), illustrate a marked reduction in P_{dimax} 14-days after C_2SH in VEH (orange circles) and SPG302 treated (blue squares) compared to SHAM rats (grey diamonds; *, $P<0.05$). However, 14-day treatement with SPG302 improved P_{dimax} in SPG302 rats compared to VEH ($^{\#}$, $P<0.05$). One-way ANOVA with Tukey's post-test, $n=7$ SHAM, $n=12$ VEH, $n=9$ SPG302.

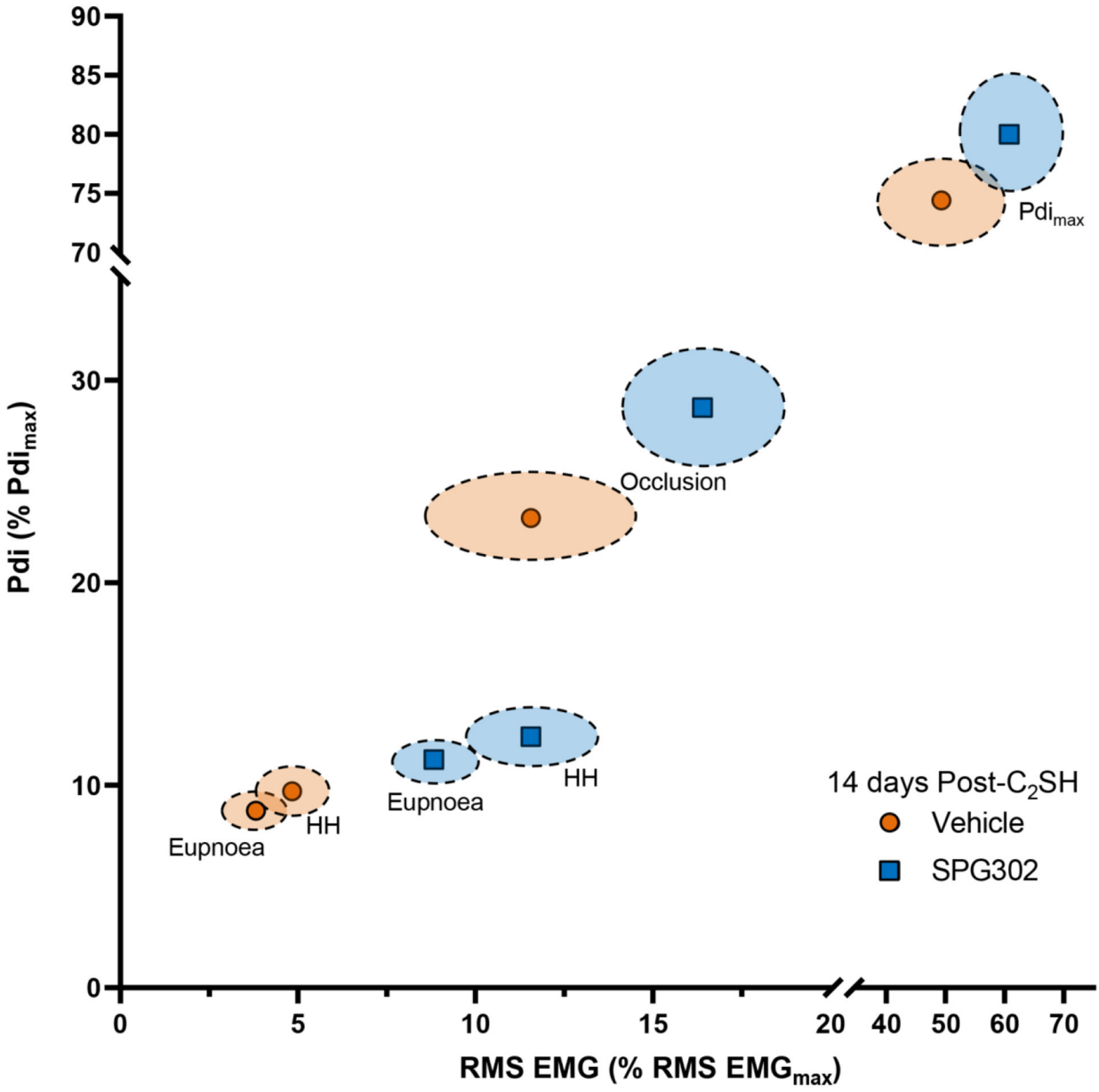

Figure 9.

Correlation of normalised P_{di} values to estmated preinjury P_{dimax} and nomalised RMS EMG (on the injured side) to RMS EMG_{max} across the gamut of ventilatory (eupnoea, HH and occlusion) and non-ventilatory behaviours 14-days post C_2SH. *XY* plot shows the linearity of increased P_{di} with increased RMS EMG with increased DIAm motor unit recruitment. Cluster analyses shows increased P_{di} and RMS EMG of SPG302 treated rats (blue squares) compared to VEH (orange circles)

Table 1:

Respiratory Parameters

Parameter		Sham (*n*=7)	Vehicle C_2SH (*n*=14)	SPG302 (*n*=10)	Two-Way ANOVA
Eupnoea Respiratory Rate (bpm)	Pre-	60 ± 16	57 ± 14	61 ± 8	Time: F=0.9; *P*=0.40 Group: F=0.3; *P*=0.75 Interaction: F=1.1; *P*=0.37
	Post-	57 ± 15	52 ± 11	62 ± 10	
	Day 14	59 ± 15	61 ± 11	60 ± 14	
Eupnoea Duty Cycle (%)	Pre-	42 ± 8	39 ± 9	40 ± 10	Time: F=1.6; *P*=0.21 Group: F=0.2; *P*=0.79 Interaction: F=0.3; *P*=0.86
	Post-	44 ± 7	44 ± 8	46 ± 10	
	Day 14	44 ± 6	41 ± 12	40 ± 8	
HH Respiratory Rate (bpm)	Pre-	71 ± 18	76 ± 19	77 ± 14	Time: F=2.0; *P*=0.12 Group: F=0.1; *P*=0.88 Interaction: F=1.3; *P*=0.30
	Post-	73 ± 17	66 ± 13	71 ± 8	
	Day 14	74 ± 17	84 ± 18	74 ± 14	
HH Duty Cycle (%)	Pre-	50 ± 10	51 ± 9	51 ± 9	Time: F=0.4; *P*=0.68 Group: F=0.1; *P*=0.88 Interaction: F=1.5; *P*=0.21
	Post-	50 ± 5	49 ± 11	52 ± 10	
	Day 14	53 ± 8	54 ± 8	50 ± 11	
Occlusion Respiratory Rate (bpm)	Pre-	31 ± 11	37 ± 8	36 ± 9	Time: F=1.1; *P*=0.36 Group: F=0.5; *P*=0.61 Interaction: F=0.4; *P*=0.80
	Post-	32 ± 6	31 ± 6	32 ± 9	
	Day 14	33 ± 11	34 ± 8	36 ± 13	
Occlusion Duty Cycle (%)	Pre-	42 ± 13	38 ± 7	38 ± 12	Time: F=0.4; P=0.65 Group: F=0.4; P=0.69 Interaction: F=0.6; P=0.69
	Post-	41 ± 13	38 ± 9	35 ± 7	
	Day 14	39 ± 8	41 ± 13	41 ± 14	

All data presented as Mean ± SD. Two-Way ANOVA

Table 2:

Contralateral DIAm RMS EMG

Parameter		Vehicle C_2SH (*n*=14)	SPG302 (*n*=10)	Three-Way ANOVA
Eupnoea (% Pre-Injury)	Post-	95 ± 29	105 ± 39	Time: F=2.2; *P*=0.15 Behaviour: F=0.3; *P*=0.71 Treatment: F=0.02; *P*=0.88 Interaction: F=0.1; *P*=0.82
	Day 14	104 ± 33	108 ± 33	
HH (% Pre-Injury)	Post-	99 ± 38	95 ± 39	
	Day 14	113 ± 42	95 ± 32	
Occlusion (% Pre-Injury)	Post-	98 ± 37	92 ± 48	
	Day 14	104 ± 53	128 ± 24	

All data presented as Mean ± SD, normalised to pre-injury values of each behaviour. Three-Way ANOVA.